

# Metallomics

Integrated biometal science

Accepted Manuscript

This article can be cited before page numbers have been issued, to do this please use: R. Dallinger, O. Zerbe, C. Baumann, B. Egger, M. Capdevila, O. Palacios, R. Albalat, S. Calatayud, P. Ladurner, B. Schlick-Steiner, F. Steiner, V. Pedrini-Martha, R. Lackner, H. H. Lindner, M. Dvorak, M. Niederwanger, R. Schnegg and S. Atrian, *Metallomics*, 2020, DOI: 10.1039/C9MT00259F.



This is an Accepted Manuscript, which has been through the Royal Society of Chemistry peer review process and has been accepted for publication.

Accepted Manuscripts are published online shortly after acceptance, before technical editing, formatting and proof reading. Using this free service, authors can make their results available to the community, in citable form, before we publish the edited article. We will replace this Accepted Manuscript with the edited and formatted Advance Article as soon as it is available.

You can find more information about Accepted Manuscripts in the [Information for Authors](#).

Please note that technical editing may introduce minor changes to the text and/or graphics, which may alter content. The journal's standard [Terms & Conditions](#) and the [Ethical guidelines](#) still apply. In no event shall the Royal Society of Chemistry be held responsible for any errors or omissions in this Accepted Manuscript or any consequences arising from the use of any information it contains.

# “Significance to metallomics”

View Article Online  
DOI: 10.1039/C9MT00259F

## Statement

In the present study we apply gastropod (snail) metallothioneins at a lineage level as model molecules, trying to track the evolution, structural / functional optimization and diversification of metal-selectivity under the persistent influence of cadmium since early gastropod evolution. To this aim, we applied an “Eco”-Metallomics approach including 74 MT sequences from 47 gastropod species, combining phylogenomic methods with molecular, biochemical, and spectroscopic techniques. This allows us to demonstrate that Cd binding selectivity paired with Cd-specific tasks has emerged repeatedly in Gastropoda clades since 430 million years. We believe that our article may be particularly significant to metallomics, because it demonstrates how differing techniques such as molecular and biochemical methods, combined with ecological and evolutionary approaches, can prove how a rare metallic trace element like cadmium has shaped the structure, metal-binding behavior and physiological function of an important protein family.

1  
2  
3  
4  
5  
6  
7  
8  
9  
10  
11  
12  
13  
14  
15  
16  
17  
18  
19  
20  
21  
22  
23  
24  
25  
26  
27  
28  
29  
30  
31  
32  
33  
34  
35  
36  
37  
38  
39  
40  
41  
42  
43  
44  
45  
46  
47  
48  
49  
50  
51  
52  
53  
54  
55  
56  
57  
58  
59  
60

1  
2  
3  
4  
5  
6  
7  
8  
9  
10  
11  
12  
13  
14  
15  
16  
17  
18  
19  
20  
21  
22  
23  
24  
25  
26  
27  
28  
29  
30  
31  
32  
33  
34  
35  
36  
37  
38  
39  
40  
41  
42  
43  
44  
45  
46  
47  
48  
49  
50  
51  
52  
53  
54  
55  
56  
57  
58  
59  
60

1  
2  
3  
4  
5  
6  
7  
8  
9  
10  
11  
12  
13  
14  
15  
16  
17  
18  
19  
20  
21  
22  
23  
24  
25  
26  
27  
28  
29  
30  
31  
32  
33  
34  
35  
36  
37  
38  
39  
40  
41  
42  
43  
44  
45  
46  
47  
48  
49  
50  
51  
52  
53  
54  
55  
56  
57  
58  
59  
60

View Article Online  
DOI: 10.1039/C9MT00259F

# Metallomics reveal a persisting impact of cadmium on the evolution of metal-selective snail metallothioneins

by

Reinhard Dallinger<sup>1,2\*</sup>, Oliver Zerbe<sup>3\*</sup>, Christian Baumann<sup>3</sup>, Bernhard Egger<sup>1</sup>, Mercé Capdevila<sup>4</sup>, Òscar Palacios<sup>4</sup>, Ricard Albalat<sup>5</sup>, Sara Calatayud<sup>5</sup>, Peter Ladurner<sup>1,2</sup>, Birgit Schlick-Steiner<sup>6</sup>, Florian Steiner<sup>6</sup>, Veronika Pedrini-Martha<sup>1</sup>, Reinhard Lackner<sup>1</sup>, Herbert Lindner<sup>7</sup>, Martin Dvorak<sup>1</sup>, Michael Niederwanger<sup>1</sup>, Raimund Schnegg<sup>1</sup>, Silvia Atrian<sup>5,†</sup>

<sup>1</sup> Department of Zoology, University of Innsbruck, Austria

<sup>2</sup> Center for Molecular Biosciences Innsbruck, Austria

<sup>3</sup> Department of Chemistry, University of Zürich, Switzerland

<sup>4</sup> Departament de Química, Universitat Autònoma de Barcelona, Spain

<sup>5</sup> Department of Genetics, University of Barcelona, Spain

<sup>6</sup> Department of Ecology, University of Innsbruck, Austria

<sup>7</sup> Division of Clinical Biochemistry, Innsbruck Medical University, Austria

<sup>†</sup> deceased. We want to dedicate this work to our longtime cooperation partner, Silvia Atrian

\* Corresponding authors: [reinhard.dallinger@uibk.ac.at](mailto:reinhard.dallinger@uibk.ac.at) and [oliver.zerbe@chem.uzh.ch](mailto:oliver.zerbe@chem.uzh.ch)

1  
2 40 **Abstract**

3  
4 41 The tiny contribution of cadmium (Cd) to the composition of the earth crust contrasts with its high  
5 42 biological significance, owing mainly to the competition of Cd with the essential zinc (Zn) for suitable  
6 43 metal binding sites in proteins. In this context it was speculated that in several animal lineages, the protein  
7 44 family of metallothioneins (MTs) has evolved to specifically detoxify Cd. Although the multi-  
8 45 functionality and heterometallic composition of MTs in most animal species does not support such an  
9 46 assumption, there are some exceptions from this role, particularly in animal lineages at the roots of animal  
10 47 evolution. In order to substantiate this hypothesis and to further understand MT evolution, we have studied  
11 48 MTs of different snails that exhibit clear Cd-binding preferences in a lineage-specific manner. By applying  
12 49 a metallomics approach including 74 MT sequences from 47 gastropod species, and by combining  
13 50 phylogenomic methods with molecular, biochemical, and spectroscopic techniques, we show that Cd  
14 51 selectivity of snail MTs has resulted from convergent evolution of metal-binding domains that  
15 52 significantly differ in their primary structure. We also demonstrate how their Cd selectivity and specificity  
16 53 has been optimized by the persistent impact of Cd through 430 million years of MT evolution, modifying  
17 54 them upon lineage-specific adaptation of snails to different habitats. Overall, our results support the role  
18 55 of Cd for MT evolution in snails, and provide an interesting example of a vestigial abiotic factor directly  
19 56 driving gene evolution. Finally, we discuss the potential implications of our findings for studies devoted  
20 57 to the understanding of mechanisms leading to metal specificity in proteins, which is important when  
21 58 designing metal-selective peptides.  
22 59  
23 60

Metallomics Accepted Manuscript

## Introduction

With a tiny amount of about 0.00001%, the contribution of cadmium (Cd) to the composition of the earth crust is seemingly negligible <sup>1</sup>. In spite of this, the biological significance of Cd is distinctly higher, owing to its particular patchy distribution, enrichment and circulation in the biosphere <sup>2</sup>. In some diatom marine algae, for example, Cd has achieved an essential importance as a constituent of the algal enzyme carbonic anhydrase, a fact that has been explained by the relative preponderance of Cd at the cost of lowly available Zn in oceanic environments inhabited by these algae <sup>3,4</sup>. In most organisms, however, Cd is highly toxic at very low concentrations, due to its physico-chemical similarity and competition with zinc (Zn) <sup>5</sup>, one of the most important essential trace elements. Because of this, most organisms have developed strategies for Cd handling and detoxification <sup>6</sup>, and it has been hypothesized that metallothioneins (MTs), a ubiquitous protein family with a high affinity to transition metal ions, may have been developed by organisms to clear this highly toxic metal <sup>7</sup>. Yet, this hypothesis has been questioned because of the apparent involvement of most MTs in a variety of functions, and their often heterometallic and metamorphic composition with binding affinities to different metal ions <sup>8-10</sup>. However, MTs form a huge and diverse gene superfamily present in most kingdoms of organisms, from bacteria through fungi, plants and animals <sup>11,12</sup>. This suggests that their origins may go back to the primal evolutionary roots of life on earth, although the metal preference of the ancestral MT remains unknown. In contrast to modern vertebrates some MTs at the roots of, for example, Chordata are Cd-selective, as recently reported for MTs of the tunicate *Oikopleura dioica* <sup>13</sup>. Cd- and Cu-selective MTs have also been discovered in several species of the ancient mollusk class of Gastropoda (snails and slugs) <sup>14,15</sup>. This suggests that in early evolution of life, Cd-selectivity of MTs might have been more common than today, and this feature has evidently been preserved to the present in diverse animal clades while it disappeared in others.

To support this hypothesis, we have taken advantage of the Cd-specific gastropod MTs, which provide an ideal model system to study the evolutionary influence of Cd on MT evolution along more of 400 million years (MY) of Gastropoda diversification. Unlike many other modern animals, snails possess metal-selective MTs, such as Cd- (CdMTs) and Cu-selective (CuMTs) isoforms <sup>15</sup> that perform Cd- or Cu-specific tasks. Thereby they exhibit a straightforward relationship between metal binding features and related physiological functions. Interestingly, Cd-specific snail MTs bind this metal with a strength and exclusive preference hardly observed in any other protein family. They are expressed in a multitude of isoforms that vary in a clade-specific manner allowing us to compare and evaluate similar proteins and protein variants (and their metal-binding modifications) in a large number of species that have adapted to different habitats. These spread from marine through terrestrial to freshwater environments with significantly different Cd concentrations. This comparative approach is central to understand how MTs have been optimized for Cd binding during gastropod evolution by the continuous impact of Cd, and how its influence is modulated by habitat-specific environmental constraints.

1  
2 96 In our work, we applied a comprehensive metalloomics approach by characterizing 74 novel or  
3 known MT sequences from 47 species across all major gastropod clades<sup>14–23</sup>. We used phylogenomic  
4 97 methods based on next generation sequencing to obtain transcriptomic data for evolutionary analyses and  
5 98 construction of phylogenetic trees. We also analyzed neutral DNA markers to compare the resulting  
6 99 phylogenetic tree with MT-derived trees. In addition, we provide data on metal-selective features of  
7 100 recombinant snail MTs and their metal-binding domains, based on molecular, biochemical and  
8 101 spectroscopic methods. Our data indicate that Cd selectivity has evolved since 430 million years ago  
9 102 (MYA) in gastropod MTs through convergent evolution of metal-binding domains with diverging primary  
10 103 structures. We study the mechanisms by which their Cd binding features have been optimized, and  
11 104 illustrate how they have diversified into different kinds with altered or even lost metal selectivity through  
12 105 lineage-specific transition into novel habitats that differ in their natural Cd background concentrations.  
13 106 Overall, we have been able to demonstrate a continuous impact of Cd on evolution of one of the most  
14 107 important metal-binding protein families, and describe a paradigmatic case of how an abiotic factor  
15 108 directly drives gene evolution. Finally, we discuss possible implications of our findings to better  
16 109 understand how metal-selectivity has been achieved in nature, and how this knowledge can help in  
17 110 designing metal-selectivity in synthetic peptides.  
18 111

## 113 **Material and methods**

### 114 **Animal collection, rearing and Cd exposure**

115 A list of gastropod species involved in experimental work for the present study along with  
116 methodical applications is reported in **Table 1**.  
117

118 Individuals of *Alinda biplicata* and *Deroceras reticulatum* were collected in suburbs of Innsbruck  
119 (Tyrol, Austria) in 2017 and 2018. Individuals of *Patella vulgata* were collected in Barcelona, Spain in  
120 summer 2016. Snails of the helicid species *Cornu aspersum* were bought from a commercial dealer  
121 (Wiener Schnecken Manufaktur, Vienna, Austria), as were the aquatic species *Marisa cornuarietis*,  
122 *Anentome helena*, *Physa acuta* and *Aplysia californica* (Aquaristikzentrum Innsbruck, Tyrol, Austria).  
123 Adult individuals of *Lottia gigantea* were collected and kindly provided to us by Dr. Douglas J. Eernisse  
124 (California State University, Fullerton, Ca, USA).  
125

126 For Cd exposure of *Cornu aspersum*, adult snails were acclimatized on garden earth substrate  
127 containing lime powder (CaCO<sub>3</sub>) in groups of 30 individuals each under stable conditions in a climate  
128 chamber (18°C, 12h light/dark cycle) and were fed regularly with uncontaminated lettuce (*Lactuca sativa*)  
129 under moistened conditions for one week. For Cd exposure, control snails were fed with uncontaminated  
130 lettuce whereas Cd-exposed snails were fed with Cd-enriched lettuce which had been incubated for one  
131

1  
2 130 hour in a CdCl<sub>2</sub>-solution containing 2 mg/l Cd<sup>2+</sup> <sup>24</sup>. After five days of exposure, five individuals of each  
3  
4 131 group were sacrificed.

View Article Online  
DOI: 10.1039/C9MT00259F

5  
6 132 Individuals of *Lymnaea stagnalis* were collected from an unpolluted freshwater pond in the  
7 133 Ternopil region, Ukraine (49°49' N, 25°23' E) and were kindly provided to us by Dr. Oksana B. Stoliar  
8  
9 134 and Dr. Halina I. Falfushynska (Ternopil National Pedagogical University, Ukraine). For metal exposure,  
10  
11 135 snails were kept in 80 l tanks of aerated tap water during 14 days, and exposed to a Cd concentration of  
12  
13 136 15 µg/l (in tap water). Water and Cd solutions were renewed every two days, lettuce feed was provided  
14  
15 137 before water exchange. Control snails without Cd addition were kept in the same manner as exposed  
16  
17 138 individuals. At the end of the exposure, three individuals per group were dissected for mRNA extraction  
18  
19 139 from midgut gland.

### 141 **Dissection, RNA/DNA isolation and cDNA synthesis**

142  
143  
144  
145  
146  
147  
148  
149  
150  
151  
152  
153  
154  
155  
156  
157  
158  
159  
160  
161  
162  
163  
164  
165  
166  
167  
168  
169  
170  
171  
172  
173  
174  
175  
176  
177  
178  
179  
180  
181  
182  
183  
184  
185  
186  
187  
188  
189  
190  
191  
192  
193  
194  
195  
196  
197  
198  
199  
200  
201  
202  
203  
204  
205  
206  
207  
208  
209  
210  
211  
212  
213  
214  
215  
216  
217  
218  
219  
220  
221  
222  
223  
224  
225  
226  
227  
228  
229  
230  
231  
232  
233  
234  
235  
236  
237  
238  
239  
240  
241  
242  
243  
244  
245  
246  
247  
248  
249  
250  
251  
252  
253  
254  
255  
256  
257  
258  
259  
260  
261  
262  
263  
264  
265  
266  
267  
268  
269  
270  
271  
272  
273  
274  
275  
276  
277  
278  
279  
280  
281  
282  
283  
284  
285  
286  
287  
288  
289  
290  
291  
292  
293  
294  
295  
296  
297  
298  
299  
300  
301  
302  
303  
304  
305  
306  
307  
308  
309  
310  
311  
312  
313  
314  
315  
316  
317  
318  
319  
320  
321  
322  
323  
324  
325  
326  
327  
328  
329  
330  
331  
332  
333  
334  
335  
336  
337  
338  
339  
340  
341  
342  
343  
344  
345  
346  
347  
348  
349  
350  
351  
352  
353  
354  
355  
356  
357  
358  
359  
360  
361  
362  
363  
364  
365  
366  
367  
368  
369  
370  
371  
372  
373  
374  
375  
376  
377  
378  
379  
380  
381  
382  
383  
384  
385  
386  
387  
388  
389  
390  
391  
392  
393  
394  
395  
396  
397  
398  
399  
400  
401  
402  
403  
404  
405  
406  
407  
408  
409  
410  
411  
412  
413  
414  
415  
416  
417  
418  
419  
420  
421  
422  
423  
424  
425  
426  
427  
428  
429  
430  
431  
432  
433  
434  
435  
436  
437  
438  
439  
440  
441  
442  
443  
444  
445  
446  
447  
448  
449  
450  
451  
452  
453  
454  
455  
456  
457  
458  
459  
460  
461  
462  
463  
464  
465  
466  
467  
468  
469  
470  
471  
472  
473  
474  
475  
476  
477  
478  
479  
480  
481  
482  
483  
484  
485  
486  
487  
488  
489  
490  
491  
492  
493  
494  
495  
496  
497  
498  
499  
500  
501  
502  
503  
504  
505  
506  
507  
508  
509  
510  
511  
512  
513  
514  
515  
516  
517  
518  
519  
520  
521  
522  
523  
524  
525  
526  
527  
528  
529  
530  
531  
532  
533  
534  
535  
536  
537  
538  
539  
540  
541  
542  
543  
544  
545  
546  
547  
548  
549  
550  
551  
552  
553  
554  
555  
556  
557  
558  
559  
560  
561  
562  
563  
564  
565  
566  
567  
568  
569  
570  
571  
572  
573  
574  
575  
576  
577  
578  
579  
580  
581  
582  
583  
584  
585  
586  
587  
588  
589  
590  
591  
592  
593  
594  
595  
596  
597  
598  
599  
600  
601  
602  
603  
604  
605  
606  
607  
608  
609  
610  
611  
612  
613  
614  
615  
616  
617  
618  
619  
620  
621  
622  
623  
624  
625  
626  
627  
628  
629  
630  
631  
632  
633  
634  
635  
636  
637  
638  
639  
640  
641  
642  
643  
644  
645  
646  
647  
648  
649  
650  
651  
652  
653  
654  
655  
656  
657  
658  
659  
660  
661  
662  
663  
664  
665  
666  
667  
668  
669  
670  
671  
672  
673  
674  
675  
676  
677  
678  
679  
680  
681  
682  
683  
684  
685  
686  
687  
688  
689  
690  
691  
692  
693  
694  
695  
696  
697  
698  
699  
700  
701  
702  
703  
704  
705  
706  
707  
708  
709  
710  
711  
712  
713  
714  
715  
716  
717  
718  
719  
720  
721  
722  
723  
724  
725  
726  
727  
728  
729  
730  
731  
732  
733  
734  
735  
736  
737  
738  
739  
740  
741  
742  
743  
744  
745  
746  
747  
748  
749  
750  
751  
752  
753  
754  
755  
756  
757  
758  
759  
760  
761  
762  
763  
764  
765  
766  
767  
768  
769  
770  
771  
772  
773  
774  
775  
776  
777  
778  
779  
780  
781  
782  
783  
784  
785  
786  
787  
788  
789  
790  
791  
792  
793  
794  
795  
796  
797  
798  
799  
800  
801  
802  
803  
804  
805  
806  
807  
808  
809  
810  
811  
812  
813  
814  
815  
816  
817  
818  
819  
820  
821  
822  
823  
824  
825  
826  
827  
828  
829  
830  
831  
832  
833  
834  
835  
836  
837  
838  
839  
840  
841  
842  
843  
844  
845  
846  
847  
848  
849  
850  
851  
852  
853  
854  
855  
856  
857  
858  
859  
860  
861  
862  
863  
864  
865  
866  
867  
868  
869  
870  
871  
872  
873  
874  
875  
876  
877  
878  
879  
880  
881  
882  
883  
884  
885  
886  
887  
888  
889  
890  
891  
892  
893  
894  
895  
896  
897  
898  
899  
900  
901  
902  
903  
904  
905  
906  
907  
908  
909  
910  
911  
912  
913  
914  
915  
916  
917  
918  
919  
920  
921  
922  
923  
924  
925  
926  
927  
928  
929  
930  
931  
932  
933  
934  
935  
936  
937  
938  
939  
940  
941  
942  
943  
944  
945  
946  
947  
948  
949  
950  
951  
952  
953  
954  
955  
956  
957  
958  
959  
960  
961  
962  
963  
964  
965  
966  
967  
968  
969  
970  
971  
972  
973  
974  
975  
976  
977  
978  
979  
980  
981  
982  
983  
984  
985  
986  
987  
988  
989  
990  
991  
992  
993  
994  
995  
996  
997  
998  
999  
1000

Snails were sacrificed and midgut gland tissue of individual snails (n = 3-5) (*Patella vulgata*, *Lottia gigantea*, *Anentome helena*, *Marisa cornuarietis*, *Aplysia californica*, *Cornu aspersum*, *Deroceras reticulatum*, *Lymnaea stagnalis*) or – due to the small size of some species – mixed tissue parts (*Alinda biplicata*, *Physella acuta*) were dissected and stored in RNAlater® (Fisher Scientific, Vienna, Austria) at -80 °C. For quantitative Real Time PCR (qPCR) after metal exposure, small aliquots of midgut gland tissue (approx. 1 mg fresh weight) of control and Cd-exposed *Cornu aspersum* and *Lymnaea stagnalis* (n = 3-5) were transferred to RNAlater® (Fisher Scientific, Vienna, Austria) whereas the remaining part of the tissue was collected for metal measurement.

RNA tissue samples were homogenized with a Precellys® homogenizer (Bertin Instruments, Montigny-le-Bretonneux, France). Total RNA was isolated using the RNeasy Plant Mini Kit (Qiagen, Hilden, Germany) including the on-column DNase I digestion according to the manufacturer's instructions (Qiagen). RNA integrity was checked by agarose gel electrophoresis and concentrations were estimated with Nanodrop (Thermo Fisher Scientific, Waltham, CA, USA). For qPCR, RNA samples were measured in triplicates with the Quant-iT™ Ribogreen® RNA Assay Kit (Life Technologies Corporation, Carlsbad, USA) applying the Victor™ X4 Multilable Reades (Perkin Elmer, Waltham, USA). 450 ng of total RNA was transcribed to cDNA in a 50 µl approach with the RevertAid Reverse Transcriptase (Thermo Fisher Scientific). For amplification of the multidomain MT sequences (*Alinda biplicata*, *Marisa cornuarietis*) AccuScript Hi-Fi Reverse transcriptase (Agilent, Santa Clara, CA, USA) was used in a 20 µl approach for cDNA synthesis.

For phylogenetic reconstruction based on neutral markers, DNA of the same specimens mentioned above was extracted using GenElute™ Mammalian Genomic DNA Miniprep Kit (Sigma Aldrich). A ~590 bp stretch of the mitochondrial gene Cytochrome C oxidase I (COI) was amplified using the standard



1  
2164 primers LCO1490 and HCO2198 suggested by <sup>25</sup> and the degenerated primers LoboF1 and LoboR1 <sup>26</sup> for  
3  
4165 some species.

View Article Online  
DOI: 10.1039/C9MT00259F

5  
6166 PCR products of *Neritina pulligera* and *Littorina littorea* showed multiple bands and therefore  
7167 were cloned before sequencing using the pTZ57R/T InsTAclone Kit (Thermo Fisher, Waltham, USA).

8  
9168 To obtain ~1000 bp of 18SrDNA the following primers of <sup>25</sup> were used in various combinations:  
10  
1169 18A1, 470F, 1155F 700R, 1500R, 1800. PCR products were purified and Sanger sequenced by the  
12  
1370 facilities of Eurofins (MWG Operon, Germany). For *Helix pomatia* and *Patella vulgate*, only ~500 bp of  
14  
1571 18SrDNA sequence were available; thus, full sequences were obtained from GenBank (FJ977750,  
16  
1772 FJ977632, AF239734, AY145373, MF544434, AY427527). Conditions for thermal cycling, polymerase  
18  
1973 and PCR are shown in **Table S1**, newly generated sequences have been deposited at GenBank  
20  
2174 (MK919674-MK919701).

### 22 2375 24 2576 **RNA seq and transcriptome assembly**

26  
2777 Isolated RNA from an individual midgut gland (*Patella vulgata*, *Neritina pulligera*, *Littorina*  
28  
2978 *littorea*, *Pomatias elegans*, *Pomacea bridgesii*, *Marisa cornuarietis*, *Anentome helena*, *Elysia crispata*,  
30  
3179 and *Limax maximus*) or of pooled soft-tissue (*Alinda biplicata*) was sent to the Duke Center for Genomic  
32  
3380 and Computational Biology (GBC, Duke University, Durham, NC, USA) and sequenced with Hi-Seq  
34  
3581 4000 Illumina sequencing. A separate library was sequenced for each species. Raw data were assembled  
36  
3782 using Trinity <sup>27</sup> version: v2.1.1 with default settings. Assemblies were provided for analysis on a local  
38  
3983 BLAST server “SequenceServer” <sup>28</sup>, where cDNA sequences encoding for diverse snail MTs were blasted  
40  
4184 against the transcriptomic data sets to identify MT sequences. Raw sequence reads data were deposited as  
42  
4385 Bioproject data base under the accession number PRJNA604693.

### 44 4586 46 4787 **Collection and processing of transcriptomic data**

48  
4988 For the species *Nacella polaris* and *Cepaea nemoralis*, raw reads from the SRA database (NCBI)  
50  
5189 were imported to Geneious R10 (Biomatters Ltd., Auckland, New Zealand) to assemble transcriptomes.  
52  
5390 New MT sequences were identified by blasting already known MT sequences from close relatives against  
54  
5591 the new transcriptomes. For most other species, MT peptide sequences of the diverse gastropod families  
56  
5792 were identified using the blastn tool at the NCBI platform (<https://blast.ncbi.nlm.nih.gov/Blast.cgi>) against  
58  
5993 the database transcriptome shotgun assembly for gastropod species (taxid: 6448).

### 60 6194 62 6395 **MT sequence confirmation via long distance (LD) PCR and quantitative Real-time PCR**

64  
6596 Gene-specific primers (**Table S2A**) were designed from identified MT sequences derived from  
66  
6797 transcriptomic data (see above). For PCR, a 50µl approach was set up using the Advantage 2 PCR System  
68  
6998 (Clontech, Takara Bio Europe, Saint-Germain-en-Laye, France) (**TableS2B**). PCR products were



1  
2199 separated on a 1.5% agarose gel (Biozym, Hessisch Oldendorf, Germany) and gene specific bands were  
3 excised. DNA was purified applying the QIAquick™ Gel Extraction Kit (Qiagen, Hilden, Germany), and  
4200 cleaned samples were sent to Microsynth AG (Balgach, Switzerland) for Sanger-sequencing. When  
5201 necessary, subsequent cloning was performed with the TOPO® TA Cloning® Kit for sequencing  
6202 (Invitrogen, Thermo Fisher Scientific, Waltham, MA, USA). Insert containing plasmids were purified  
7203 using the QIAprep Spin Miniprep Kit (Qiagen, Hilden, Germany) and sent to Microsynth AG (Balgach,  
8204 Switzerland) for Sanger sequencing. Primer design and sequence analysis were performed applying CLC  
9205 Main workbench 6.9 (Quiagen, Aarhus, Denmark).

10206  
11207 For CdMT quantification of *Cornu aspersum*, cDNA of the controls and Cd-exposed individuals  
12208 were measured in triplicates using a 7500 Real Time PCR Analyzer with Power SYBR® Green detection  
13209 (Applied Biosystems™ by ThermoFisher Scientific, USA). Details on primer design and concentrations  
14210 as well as establishment of the calibration curve are described in <sup>26</sup>. Total RNA was used as a reference  
15211 for transcriptional quantification (see <sup>29</sup>).

### 16212 17213 **Phylogenetic analysis**

18214 Alignments of MT amino acid sequences were done with MUSCLE v3.8.31 <sup>30</sup>, and manual  
19215 corrections were applied if deemed appropriate. Alignment length was variable and species-specific, with  
20216 protein lengths between 50 and 180 amino acids. All alignments applied for the present tree calculations  
21217 are reported as FASTA alignments (see **Alignments S1-5**). Phylogenetic tree reconstructions were  
22218 performed with RAxML v8.2.8 (maximum likelihood ML, <sup>31</sup>) and MrBayes v3.2.6 (Bayesian inference  
23219 BI, <sup>32</sup>). For ML with the model PROTGAMMAIWAG, 1000 - 10,000 inferences were calculated, and  
24220 1,000 bootstrap replicates. For BI, 10 million generations were calculated with rates=invgamma and  
25221 aamodelpr=mixed, average standard deviation of split frequencies.

26222 In addition, phylogenetic trees were also computed with a maximum likelihood (ML) approach  
27223 with 500 bootstrap replicates, using the freely accessible programme platform SeaView (version 4.7) of  
28224 PRABI-Doua, using default settings. Overall topologies between BI and ML trees were very similar, and  
29225 the trees with the lowest number of polytomies are shown.

30226 Mitochondrial COI sequences were manually aligned and checked for correct amino acid  
31227 translation; the ribosomal 18SrDNA sequences were aligned using the SINA Alignment tool v. 1.2.11,  
32228 based on the SILVA database <sup>33</sup> (**Alignment S1**). In all phylogenetic reconstructions gaps were treated as  
33229 missing data. Four partitions were defined in the concatenated data, one for each codon position of COI  
34230 and one for 18SrDNA. ML analysis was performed using IQ-tree <sup>34</sup> allowing for model estimation in each  
35231 partition; node supports were calculated using 1000 non-parametric UltraFast Bootstraps. For BI the best-  
36232 fitting substitution models were obtained with Modeltest 3.7. <sup>35</sup>: GTR+I+G achieved the best AIC and  
37233 BIC values in all four partitions. BI was performed with MrBayes v3.2.6 allowing for unlinked parameter

1  
234 estimation in each partition. Five million generations were performed and 25% burnin was chosen to  
3  
235 discard data prior to convergence of runs (standard deviation of split-frequencies below 0.01). The MF  
4  
5  
236 tree and the BI tree (data not shown) revealed the same topology.

### 238 **Cloning and recombinant expression of *MT* genes from *Pomacea bridgesii* and *Lottia gigantea***

10  
239 Full-length synthetic cDNAs for *PbMT1* and *LgMT1* genes were synthesized by Integrated DNA  
12  
240 Technologies Company (Coralville, IA, USA) and by Synbiotech (Monmouth Junction NJ, USA),  
13  
14  
241 respectively. Both cDNAs were cloned into the *E. coli* pGEX-4T-1 expression vector (GE Healthcare) as  
15  
242 described elsewhere<sup>13</sup> with minor modifications. Cloned *PbMT1* and *LgMT1* cDNAs were sequenced  
16  
243 with the Big Dye Terminator v3.1 Cycle Sequencing Kit (Applied Biosystems) at the Scientific and  
17  
244 Technological Centers of the University of Barcelona (ABIPRISM 310, Applied Biosystems).

18  
245 For heterologous expression of GST-MT fusion proteins, 500 mL of LB medium with 100  $\mu\text{g mL}^{-1}$   
19  
246 ampicillin were inoculated with protease-deficient *E. coli* BL21 cells previously transformed with the  
20  
247 *PbMT1* pGEX-4T-1 or *LgMT1* pGEX-4T-1 recombinant plasmids. After overnight growth at 37 °C/250  
21  
248 rpm, the cultures were used to inoculate 5 L of fresh LB-100  $\mu\text{g mL}^{-1}$  ampicillin medium. Gene expression  
22  
249 was induced with 100  $\mu\text{M}$  isopropyl- $\beta$ -D-thiogalactopyranoside (IPTG) for 3 hours (h). After the first 30  
23  
250 minutes (min) of induction, cultures were supplemented with  $\text{ZnCl}_2$  (300  $\mu\text{M}$ ),  $\text{CdCl}_2$  (300  $\mu\text{M}$ ) or  $\text{CuSO}_4$   
24  
251 (500  $\mu\text{M}$ ) in order to generate metal–MT complexes. Cells were harvested by centrifugation for 5 min at  
25  
252 9100 g (7700 rpm), and bacterial pellets were suspended in 125 mL of ice-cold PBS (1.4 M NaCl, 27 mM  
26  
253 KCl, 101 mM  $\text{Na}_2\text{HPO}_4$ , 18 mM  $\text{KH}_2\text{PO}_4$  and 0.5% v/v  $\beta$ -mercaptoethanol). Resuspended cells were  
27  
254 sonicated (Sonifier Ultrasonic Cell Disruptor) 8 min at voltage 6 with pulses of 0.6 seconds, and then  
28  
255 centrifuged for 40 min at 17200 g (12000 rpm) and 4° C.

### 257 **Purification of recombinant metal-MT complexes**

258 Protein extracts containing GST–*PbMT1* or GST–*LgMT1* fusion proteins were incubated with  
259 glutathione sepharose beads (GE Healthcare) for 1 h at room temperature with gentle rotation. GST–MT  
260 fusion proteins bound to the sepharose beads were washed with 30 mL of cold 1xPBS bubbled with argon  
261 to prevent oxidation. After three washes, GST–MT fusion proteins were digested with thrombin (GE  
262 Healthcare, 25 U L<sup>-1</sup> of culture) overnight at 17 °C, thus enabling separation of the metal–MT complexes  
263 from the GST that remained bound to the sepharose matrix. The eluted metal–MT complexes were  
264 concentrated with a 3 kDa Centriprep Low Concentrator (Amicon, Merck), and fractionated on a Superdex-  
265 75 FPLC column (GE Healthcare) equilibrated with 20 mM Tris–HCl, pH 7.0, and run at 0.8 mL min<sup>-1</sup>.  
266 The protein-containing fractions, identified by their absorbance at 254 nm, were pooled and stored at -80  
267 °C until use.

## Analysis of recombinantly expressed metal-MT complexes

For determination of the molecular mass of the metal complex species in solution, the metal-MT complexes produced by recombinant expression were analyzed by electrospray ionization mass spectrometry (ESI-MS). For that purpose, a Micro Tof-Q Instrument (Bruker Daltonics GmbH, Bremen, Germany) with a time-of-flight analyzer (ESI-TOF MS) was utilized, calibrated with ESI-L Low Concentration Tuning Mix (Agilent Technologies, Santa Clara, CA, USA), and interfaced with a Series 1100 HPLC pump (Agilent Technologies) equipped with an autosampler, both controlled by the Compass Software. The experimental conditions for analysis of Zn and Cd proteins were as follows. 10-20  $\mu\text{L}$  of the sample were injected at 40  $\mu\text{L}/\text{min}$  using the capillary-counter electrode voltage at 5.0 kV and the desolvation temperature in the 90-110  $^{\circ}\text{C}$  range. For Cu containing samples the conditions used were milder, applying the capillary-counter electrode voltage at 4.0 kV and the desolvation temperature at 80  $^{\circ}\text{C}$ . Spectra were collected throughout an  $m/z$  range from 800 to 2500. The liquid carrier was a 90:10 mixture of 15 mM ammonium acetate and acetonitrile, pH 7.0. All samples were injected in duplicates to ensure reproducibility.

## NMR and metal titration

Fully cadmium-loaded forms of *Littorina littorea* and *Helix pomatia* MTs were produced by recombinant expression and uniformly  $^{15}\text{N}$ -labelled in *E. coli* cells as described previously<sup>20</sup>. To demetallate the proteins their solutions were acidified in three buffer exchange steps, adding demetallation solutions (pH 2.0, 10 or 20 mM MES or TRIS, 10 mM TCEP) using Amicon Ultra 3K Centrifugal Filter Devices (EMD Millipore). All solutions were carefully purged with argon prior to use. Titrations were performed in 20 or 50 mM MES (pH 6.0), MES (pH 7.0) and Tris (pH 7.0) buffers with 10 mM TCEP yielding very similar results. Metallation was followed by recording [ $^{15}\text{N}$ ,  $^1\text{H}$ ]-HSQC spectra or best-type [ $^{15}\text{N}$ ,  $^1\text{H}$ ]-HSQC spectra<sup>36</sup>. Spectra were analyzed and peaks integrated applying the program CcpNmr v.2.4.2.<sup>37</sup>

Measurements of  $^{15}\text{N}$  transverse relaxation rates (R2) were performed using a HSQC-type version of the Carr Purcell Meiboom Gill (CPMG) experiment<sup>38</sup>. 32 scans were performed per increment and T2 delays of 0, 17, 34, 51, 68, 102, 119, 204 and 305 ms were used. The relaxation delay in all these experiments was set to 2 s. Spectra were recorded using Zn<sub>6</sub>- or Cd<sub>6</sub>-HpMT and Zn<sub>9</sub>- or Cd<sub>9</sub>-LIMT samples. Zn-loaded MTs were generated by adding Zn to demetallated MTs. Peaks were integrated batchwise using the program SPSCAN and R2 rates extracted from least square fits to the standard exponential decay function with gnuplot.

All spectra were recorded at 298 K on a Bruker NEON 600 MHz or 700 MHz NMR spectrometer using a PRODIGY triple-resonance probe for samples at a concentration range of 0.1- 0.5 mM.

## Tissue sample digestion and metal analyses

For Cd analysis, midgut gland tissue samples and lettuce leaves (*Lactuca sativa*) were oven-dried at 60°C. After dry weight (d.w.) determination, samples were wet-digested at 70°C with a mixture of HNO<sub>3</sub> (suprapur, Merck, Darmstadt, Germany) and deionized water (1:1) in 12 ml screw-capped polyethylene tubes (Greiner, Kremsmünster, Austria). For complete oxidation, a few drops of H<sub>2</sub>O<sub>2</sub> were added to the hot digested samples. They were filled up with deionized water to a final volume of 11.5 ml. Cd concentrations were measured by flame (Model 2380, Perkin Elmer, Boston, MA) or graphite furnace atomic absorption spectrophotometry with polarized Zeeman background correction (Model Z-8200, Hitachi, Japan) and Pd(NO<sub>3</sub>)<sub>2</sub> as a matrix modifier, depending on concentration levels in the samples. Calibration was performed with diluted titrisol standard solutions (Merck) prepared with de-ionized water and 5% HNO<sub>3</sub> (suprapur, Merck). Lobster hepatopancreas powder (TORT-2, National Research Council, Canada) was used as a standard reference material and processed in the same way as the samples (n = 5).

## Preparation and chromatography of *in vivo* MTs

Purification and preparation of *in vivo* MTs for determination of molar metal ratios were performed on centrifuged supernatants of midgut gland homogenates obtained from Cd-exposed snails (*Helix pomatia*, *Cornu aspersum*) and slugs (*Arion vulgaris*), by applying successive fractionation steps on gel permeation chromatography, anion exchange chromatography, ultrafiltration and Reverse phase HPLC<sup>23</sup>. For each species, HPLC fractions of the eluted MT peak were pooled and diluted 1:10 with deionized water under addition of 1% HNO<sub>3</sub>. Metal concentrations (Cd, Cu, Zn) were analysed in triplicate in 1 ml aliquots by graphite furnace atomic absorption spectrophotometry with polarized Zeeman background correction (Model Z-8200, Hitachi, Japan) as described above.

## Statistics

Data from q-RT-PCR and metal analyses were evaluated using SigmaPlot 12.5 (SYSTAT software, San Jose, CA, USA). Values were tested for normal distribution with the Shapiro–Wilk normality test and the equal variance test. Outliers of normally distributed data were assessed with the Grubbs test (<https://www.graphpad.com/quickcalcs/Grubbs1.cfm>). For not normally distributed data, non-parametric methods (Mann-Whitney U test) were applied. Significance levels were set at  $p \leq 0.05$ .

## Results and Discussion

In this work we propose that Cd acts as a driver in the evolution of gastropod metallothioneins. In what follows we first describe the variety of gastropod MTs (section 1), structural features of MTs (section 2), and our phylogenetic analysis of how gastropod MTs changed during evolution to gain (section 3) or

1  
2338 loose (section 4) Cd-binding selectivity. Moreover, we describe how Cd-selectivity was achieved during  
3 evolution (section 5) and conclude with how changes in environmental Cd levels influenced Cd-selectivity  
439 (section 6).  
5  
6340  
7341  
8

## 942 1. Gastropod diversity

10  
11343 Modern Gastropoda represent five distinct clades with about 80,000 species: Patellogastropoda,  
12 Neritimorpha, Vetigastropoda, Caenogastropoda and Heterobranchia. Their phylogenetic relationships  
1325,39–44 served as a reference for this study. Interestingly, several gastropod lineages have independently  
145 abandoned marine realms and successfully adapted to semi-terrestrial, terrestrial and freshwater  
146 environments<sup>45</sup>. This manifold colonization of non-marine habitats has promoted the huge diversity of  
147 gastropod traits, including the structural and functional diversity of their *MT* genes and proteins. Species  
148 and their MT sequences used for phylogenetic tree constructions of the present study are reported in **Table**  
149 **S3**.  
150  
151

## 152 2. Gastropod MTs: Structures, domain organization and metal binding features

153 Examples of primary MT structures across all major gastropod clades are shown in **Figure 1A-E**.  
154 Amino acid sequences of most gastropod MTs reflect a bipartite organization of one N-terminal metal-  
155 binding domain linked to a distinctly different C-terminal metal-binding domain (**Figure 1A, B, E**). This  
156 kind of structural organization has been confirmed by NMR studies and molecular modeling<sup>16,46</sup>. It is  
157 therefore assumed that the primordial gastropod MT was a bidominal MT. Both N-terminal and C-  
158 terminal domains, contain nine Cys residues each which bind in a stoichiometric ratio, three divalent  
159 (mainly Cd<sup>2+</sup>, Zn<sup>2+</sup>), or six monovalent (mainly Cu<sup>+</sup>) metal ions, such that a prototypical two-domain snail  
160 MT can accommodate six divalent or 12 monovalent metal ions, respectively<sup>14</sup>. An exception from this  
161 rule is observed in MTs of Patellogastropoda such as *Lottia gigantea* and *Patella vulgata*, which possess  
162 a deviating N-terminal domain that contains 10 instead of nine Cys residues, most of them arranged in  
163 form of double (Cys-Cys) motifs (**Figure 1B**). In addition to this, the N-terminal MT domain in some  
164 snail species has been duplicated once or several times independently, as seen in *Littorina littorea* and  
165 *Pomatias elegans*<sup>16,20</sup> (**Figure 1B**). In the land snail *Alinda biplicata* and in some other species, tandem  
166 duplications generated multi-domain MTs (md-MTs) consisting of modular strings of up to nine N-  
167 terminal domain repeats, always linked to a single C-terminal domain that has, to the best of our  
168 knowledge, never been duplicated<sup>47</sup> (**Figure 1C**). Domain duplications were also reported from bivalve  
169 MTs<sup>48</sup>, which have probably emerged independently from those in gastropods. In gastropods, md-MTs  
170 can bind additional metal ions according to the number of added domains within the protein chain. For  
171 example, in the three-domain MT of *Littorina littorea*, the metal binding ratio for Cd<sup>2+</sup> has been  
172 extended to a number of nine Cd<sup>2+</sup> ions as compared with six Cd<sup>2+</sup> ions in normal bidominal snail MTs



1  
2  
3  
4  
5  
6  
7  
8  
9  
10  
11  
12  
13  
14  
15  
16  
17  
18  
19  
20  
21  
22  
23  
24  
25  
26  
27  
28  
29  
30  
31  
32  
33  
34  
35  
36  
37  
38  
39  
40  
41  
42  
43  
44  
45  
46  
47  
48  
49  
50  
51  
52  
53  
54  
55  
56  
57  
58  
59  
60  
61  
62  
63  
64  
65  
66  
67  
68  
69  
70  
71  
72  
73  
74  
75  
76  
77  
78  
79  
80  
81  
82  
83  
84  
85  
86  
87  
88  
89  
90  
91  
92  
93  
94  
95  
96  
97  
98  
99  
100  
101  
102  
103  
104  
105  
106  
107  
108  
109  
110  
111  
112  
113  
114  
115  
116  
117  
118  
119  
120  
121  
122  
123  
124  
125  
126  
127  
128  
129  
130  
131  
132  
133  
134  
135  
136  
137  
138  
139  
140  
141  
142  
143  
144  
145  
146  
147  
148  
149  
150  
151  
152  
153  
154  
155  
156  
157  
158  
159  
160  
161  
162  
163  
164  
165  
166  
167  
168  
169  
170  
171  
172  
173  
174  
175  
176  
177  
178  
179  
180  
181  
182  
183  
184  
185  
186  
187  
188  
189  
190  
191  
192  
193  
194  
195  
196  
197  
198  
199  
200  
201  
202  
203  
204  
205  
206  
207  
208  
209  
210  
211  
212  
213  
214  
215  
216  
217  
218  
219  
220  
221  
222  
223  
224  
225  
226  
227  
228  
229  
230  
231  
232  
233  
234  
235  
236  
237  
238  
239  
240  
241  
242  
243  
244  
245  
246  
247  
248  
249  
250  
251  
252  
253  
254  
255  
256  
257  
258  
259  
260  
261  
262  
263  
264  
265  
266  
267  
268  
269  
270  
271  
272  
273  
274  
275  
276  
277  
278  
279  
280  
281  
282  
283  
284  
285  
286  
287  
288  
289  
290  
291  
292  
293  
294  
295  
296  
297  
298  
299  
300  
301  
302  
303  
304  
305  
306  
307  
308  
309  
310  
311  
312  
313  
314  
315  
316  
317  
318  
319  
320  
321  
322  
323  
324  
325  
326  
327  
328  
329  
330  
331  
332  
333  
334  
335  
336  
337  
338  
339  
340  
341  
342  
343  
344  
345  
346  
347  
348  
349  
350  
351  
352  
353  
354  
355  
356  
357  
358  
359  
360  
361  
362  
363  
364  
365  
366  
367  
368  
369  
370  
371  
372  
373  
374  
375  
376  
377  
378  
379  
380  
381  
382  
383  
384  
385  
386  
387  
388  
389  
390  
391  
392  
393  
394  
395  
396  
397  
398  
399  
400  
401  
402  
403  
404  
405  
406  
407

20,22. Apart from this, N- and/or C-terminal domains are modified in some species by deletions at specific positions or through premature chain truncations (**Figure 1 D,E**).

View Article Online  
DOI: 10.1039/C9MT00259F

Across all gastropod MTs, primary structures of C-terminal domains appear to be higher conserved compared with N-terminal domains. A BLAST comparison of the N-terminal domain of *Littorina littorea* with those of all other gastropod CdMTs reveals low degrees of homology in a clade-specific gradation from Heterobranchia through Caenogastropoda to Patellogastropoda (**Figure 2**). In contrast, similarity scores between C-terminal domains of the same MT sequences are much more significant. This clearly demonstrates the higher degree of conservation of C-terminal against N-terminal metal binding domains, which is also confirmed by a distance matrix derived from single domain alignments (**Table S4**). We used *Littorina littorea* as a reference because this species possesses a well characterized CdMT<sup>20,22</sup> and occupies a central position between ancient and modern Gastropoda<sup>41</sup>.

The higher evolutionary pressure for sequence conservation of the C-terminal domain in snail MTs is probably related to preferred Cd<sup>2+</sup> loading into that part of the protein. This is demonstrated by NMR data of experiments, in which Cd<sup>2+</sup> equivalents were added stepwise to the apo-MT of *Littorina littorea* (**Figure 3**). Unlike the Cd-loaded MT (**Figure 3B**), the apo-MT is unfolded and does not assume a specific three-dimensional shape (**Figure 3A**)<sup>11,49</sup>. Added Cd<sup>2+</sup> is initially cooperatively incorporated into the C-terminal domain to build the C-terminal cluster (**Figure 3C**), before the two N-terminal domains form simultaneously (**Figure 3D**). This proves a clear priority for Cd<sup>2+</sup> uptake into the C-terminal domain.

So far, the tertiary structure of two snail MTs has been disclosed by solution NMR, namely for the bidominal CdMT of the Roman snail, *Helix pomatia*<sup>46</sup>, and for the three-domain CdMT of the periwinkle, *Littorina littorea*<sup>20</sup>. The tertiary structure of the Roman snail CdMT in its dumbbell shape resembles the very similar structures of vertebrate MTs<sup>50,51</sup>. However, the metal-binding stoichiometry of the snail MT with six Cd<sup>2+</sup> ions for the entire protein and three Cd<sup>2+</sup> ions coordinated by nine Cys residues within each of the two domains, respectively, differs from the well-known metal binding stoichiometry of MTs from most other animal clades<sup>46</sup>. In mammalian MTs, four divalent metal ions are coordinated by 11 Cys residues in the C-terminal cluster (called alpha domain), whereas three divalent metal ions are bound by nine Cys residues in the N-terminal domain (called beta domain)<sup>51</sup>. The MT of *Littorina littorea* is the first reported animal MT ever that exhibits a three-domain partition<sup>20</sup>.

Many snail MTs possess Cd- or Cu-selective binding preferences, and can be isolated as stable, homometallic metal complexes from native snail tissues<sup>14,52</sup>. Although the exact prerequisites for metal-selectivity are not yet fully understood, it appears that the frequency and position of certain non-coordinating amino acid residues in the primary sequence and their spatial arrangement in the tertiary structure are crucial determinants in conferring metal-selectivity to snail MTs<sup>15,19–21</sup>.

The homometallic composition of metal-selective snail MTs was demonstrated by electrospray ionization mass spectrometry (ESI-MS) in recombinantly expressed and purified MT proteins<sup>15,22</sup>.



1  
208 Thereby, metal-selective MTs can be detected as homometallic complexes with their cognate metal ions  
3 (mainly Cd<sup>2+</sup> or Cu<sup>+</sup>) but appear as a heterometallic mixture of complexes with variable stoichiometry  
409 when forced to associate with non-cognate metal species<sup>15,18</sup>. In contrast, metal-unspecific snail MTs  
5  
6  
7410 form heterometallic mixtures of complexes with variable stoichiometry in presence of any metal ions<sup>17</sup>.  
8  
9412 According to this definition, it appears that Cd-selective MTs have not equally evolved in all gastropod  
10  
11413 clades. For example, vetigastropod species like *Megathura crenulata* possess an unspecific MT that  
12  
13414 produces a mixture of sulfide containing heterometallic complexes with reduced stability when  
1415 recombinantly expressed in Cd-enriched media<sup>17</sup> (**Figure 4**). In contrast, recombinant CdMTs of some  
16  
17416 Caenogastropoda (like *Littorina littorea*) and Heterobranchia (like *Helix pomatia*) form homometallic  
18  
19417 Cd<sup>2+</sup> complexes (**Figure 5**). MTs of Patellogastropoda are also Cd-selective. However, because of the  
20  
21418 divergent primary structure of their N-terminal domain with 10 Cys residues (**Figure 1B**), CdMTs of  
22  
23419 Patellogastropoda bind seven instead of six Cd<sup>2+</sup> ions per protein molecule, as demonstrated for *Lottia*  
24  
25420 *gigantea* (**Figure 5**). CdMTs of *Helix pomatia* and *Arion vulgaris* (Heterobranchia) bind six Cd<sup>2+</sup> ions per  
26  
27421 protein molecule or nine Cd<sup>2+</sup> ions in three-domain CdMTs like that of *Littorina littorea*  
28  
29422 (Caenogastropoda) (**Figure 5**). All gastropod CdMTs are incapable to form homometallic Cu<sup>+</sup> complexes  
30  
31423 (**Figure 5**). However, due to the chemical similarity between Zn and Cd, some recombinant gastropod  
32  
33424 CdMTs can form homometallic complexes with divalent Zn<sup>2+</sup> ions. This Zn<sup>2+</sup>-binding selectivity is low  
34  
35425 in CdMTs of Patellogastropoda, as demonstrated for *Lottia gigantea* (**Figure 5**). In contrast, Zn preference  
36  
37426 is high for Caenogastropoda CdMTs (*Littorina littorea*) and Stylommatophora CdMTs (*Helix pomatia*  
38  
39427 and *Arion vulgaris*), which are able to form homometallic Zn<sup>2+</sup> complexes in the presence of excessive  
40  
41428 Zn<sup>2+</sup> concentrations, with the same stoichiometry as for Cd<sup>2+</sup> (**Figure 5**). Interestingly, some evidence  
42  
43429 indicates Zn specificity in MTs of some mussels (Bivalvia), the mollusk sister class of gastropods<sup>44</sup>.

### 431 3. Phylogeny suggests convergent evolution of CdMTs in early gastropod clades

432 The multitude of published and collected primary MT sequences from species across all clades of  
433 Gastropoda (see **Table S3**) and basic knowledge about their structure and metal-binding features (see  
434 above) fosters an attempt towards establishing a phylogeny of gastropod MTs and, in particular, Cd-  
435 selective snail MTs. The smallness of most MT proteins and the fact that the abundance of conserved  
436 cysteine residues and repeat motifs do not bear much phylogenetically evaluable information creates a  
437 challenge in such an analysis. In the present study, we have developed a domain and metal-specific  
438 approach to compensate somewhat for these handicaps.

439 Yet, confronting a phylogeny of neutral DNA markers with one based on Cd-selective MTs  
440 (**Figure 6**) reflects the evolution of Cd selectivity in MTs of three gastropod clades: Patellogastropoda,  
441 Caenogastropoda and Heterobranchia. It appears that Cd-selective MTs are predominantly observed in  
442 species that have adapted to littoral and terrestrial environments (**Figure 6**). A closer phylogenetic view

in which MTs of Panpulmonata (a taxon of Heterobranchia comprising the lineages of Sacoglossa, Syphonariodea, Hygrophila and Stylommatophora)<sup>53</sup> are rooted with MTs of Caenogastropoda (Figure 7) reveals the loss of Cd-selective MTs in freshwater snails of Caenogastropoda and Heterobranchia, and the initial emergence and subsequent loss of Cu-selective MT isoforms (CuMTs) in the lineage of Stylommatophora (terrestrial snails and slugs). In that context it is of interest that it was previously shown that snail CuMTs are involved in Cu regulation, possibly linked to hemocyanin synthesis<sup>54,55</sup>.

Chronograms show that Cd selectivity developed from ancestral MTs twice independently. CdMTs evolved first in Patellogastropoda, about 430 million years (My) ago (Figure 8A). A second line of CdMTs emerged in the two sister clades Caenogastropoda and Heterobranchia, before 418 My ago (Figure 8A). Apart from the phylogenetic evidence, another clear indication of this independent evolution is the emergence of a new kind of N-terminal metal-binding domain in CdMTs of Patellogastropoda (see above), which differs fundamentally from N-terminal domains in CdMTs of all other gastropod lineages (Figure 1B). The two sister clades Caenogastropoda and Heterobranchia have shaped their CdMTs through parallel evolution (Figure 8A, B). This is reflected by sequence similarities and homologous domain organization across primary structures of their CdMTs (Figure 1B).

Also indicated in the chronogram are some of the main mass extinction events through the evolutionary history of the earth (Figure 8B). Fluctuating emissions of Cd through continental and super-volcanic emissions in combination with these catastrophic extinction events<sup>2,56–59</sup> may have triggered convergent evolution of Cd-selective MTs in gastropod clades since 430 My ago (Figure 8B). Evidence for increased Cd emissions through geological eras is provided by elevated Cd concentrations in worldwide bedrock formations of different geological origin, from Paleozoic<sup>60–63</sup> through Mesozoic<sup>63,64</sup> and Cenozoic<sup>65</sup>.

Based on experimental data with recombinant proteins<sup>17</sup>, it appears that Cd selectivity is lacking in MTs of Vetigastropoda (Figures 8A), which forms a sister clade to Patellogastropoda<sup>43</sup>. The metal-specific character in MTs of Neritimorpha, on the other hand, is still unknown (Figure 8A). Since Neritimorpha from a sister clade to Caenogastropoda and Heterobranchia<sup>43</sup>, it could be speculated that they share Cd-specific features with their two sister clades. On the other hand, a high degree of identity in primary sequence and domain organization between MTs of Vetigastropoda and Neritimorpha (Figure 1A) suggests the possibility that Neritimorpha MTs share some of their metal-binding features with those of Vetigastropoda. Future experiments through recombinant expression and ESI-MS analyses will probably resolve this question. The supposed zinc (Zn) specificity in MTs of some mussels (Bivalvia), the mollusk sister class of gastropods, is also indicated in Figure 8A. However, this evidence is scarce, being derived from one single experimental study<sup>44</sup>.

#### 4. Diversification and loss of cadmium selectivity during late gastropod radiation

1  
278 Since the Cretaceous period, Cd selectivity of MTs was apparently lost in snail lineages that  
3 adapted to freshwater habitats. Accordingly, metal-binding features of MTs from *Pomata bridgesii*  
479 (family of Ampullariidae, Caenogastropoda) and *Biomphalaria glabrata* (Hygrophila, Heterobranchia)  
5 (family of Ampullariidae, Caenogastropoda) and *Biomphalaria glabrata* (Hygrophila, Heterobranchia)  
6 resemble those of the unspecific *Megathura crenulata* MT<sup>17</sup> (**Figure 4**). As indicated by their primary  
7 sequence and domain organization (**Figure 1D, E**), a loss of Cd selectivity may also have occurred in  
8 caenogastropod species of freshwater Calyptridae and Buccinidae (**Figure 6**). The loss of Cd selectivity  
982 in these MTs is a derived character (**Figure 7**), suggesting that metal selectivity was no longer required in  
10 MTs of freshwater snails. In some freshwater species of Caenogastropoda such as *Pomacea canaliculata*,  
11 MTs have developed N-terminal repeats, similar to some snail CdMTs (**Figure 1C**).  
12  
13

1485  
1486  
1487 In terrestrial snails of Stylommatophora (Heterobranchia), gene duplications of the primordial  
1488 CdMT led to the emergence of three MT isoforms, each of them devoted to different, metal-specific tasks  
1489<sup>14,55,66</sup>. First, a gene duplication of *CdMT* gave rise to Cu-selective MTs, which form homometallic Cu<sup>+</sup>  
1490 complexes at a ratio of 12 Cu<sup>+</sup> ions per protein molecule, but neither bind Cd<sup>2+</sup> nor Zn<sup>2+</sup> (**Figure S1, S2**).  
1491 In a second event of gene duplication, *CuMT* genes lost their Cu selectivity in the so-called CdCuMT  
1492 isoforms<sup>18,19,55,66–68</sup> (**Figure S1 S2**). Phylogenetic trees (**Figure S3**) support the chronological succession  
1493 of these evolutionary steps.  
1494  
1495

## 1496 5. Evolutionary optimization of Cd selectivity and specificity

1497 For the sake of clarity, we like to distinguish between Cd (or metal) selectivity and specificity of  
1498 MTs. We define Cd *selectivity* as the binding preference of an MT for Cd<sup>2+</sup> ions in presence of other metal  
1499 ions, mainly Zn<sup>2+</sup> and Cu<sup>+</sup>. We define Cd (or metal) *specificity* as the involvement of the respective MT  
1500 into a Cd- or metal-specific physiological function, which is often the consequence of its metal binding  
1501 selectivity. For example, Cd-selective snail MTs are predominantly involved in Cd-specific functions like  
1502 detoxification<sup>14,69,70</sup>.

1503 Accordingly, we can observe that during gastropod evolution both, metal selectivity and  
1504 physiological specificity of snail CdMTs have been optimized in favor of Cd<sup>2+</sup>. The CdMT of *Littorina*  
1505 *littorea*, for example, has been optimized for Cd<sup>2+</sup> complexation to the disadvantage of Zn<sup>2+</sup> binding. This  
1506 can be concluded indirectly from the better fit of the protein backbone to the Cd vs the Zn cluster. To this  
1507 end we measured <sup>15</sup>N dynamics NMR data that probe for rigidity of the polypeptide backbone. Transverse  
1508 relaxation (R2) rates of Zn<sup>2+</sup>-loaded CdMTs are increased by 14 and 8 Hz in the N-terminal N1 and N2  
1509 domains of the CdMT of *Littorina littorea*, respectively, and by up to 5 Hz in the C-terminal domain of  
1510 the *Helix pomatia* CdMT (**Figure 9**) when compared to the Cd<sup>2+</sup>-loaded forms. The increase in transverse  
1511 relaxation rates reflects additional contributions from conformational exchange only for the Zn<sup>2+</sup> species,  
1512 indicating that the complexes with the cognate Cd<sup>2+</sup> ion are conformationally more stable (**Figure 9**).  
Similarly, NMR studies of the CdMT of *Helix pomatia* indicate a structural optimization for Cd<sup>2+</sup> rather

1  
2 13 than Zn<sup>2+</sup> binding<sup>46</sup>. Further evidence for an evolutionary optimization for Cd binding in these MTs comes  
3 from the fact that Cd<sup>2+</sup> ions are incorporated into these proteins cooperatively (**Figure 3**). The fact that  
4 14 peaks in the [<sup>15</sup>N,<sup>1</sup>H]-HSQC spectra occur at the same positions as in the fully-metallated domains  
5 15 indicates that no partially metallated domains form in situations of substoichiometric metal content.  
6 16 Strikingly, the Cd-selective character of gastropod CdMTs is also maintained in the presence of Cu<sup>+</sup> ions  
7 17 at equimolar concentrations with Cd<sup>2+</sup>, as demonstrated recently for the recombinantly produced CdMT  
8 18 (AvMT1) of the terrestrial slug, *Arion vulgaris*<sup>23</sup>. This is remarkable since the evolution of thiolate  
9 19 proteins with an apparent preference for binding Cd<sup>2+</sup> over Cu<sup>+</sup> is a particular feature of snail CdMTs  
10 20 which is otherwise not observed in other animal MTs<sup>46,50,51</sup>, and seems to contradict the chemical rules  
11 21 of the Irving Williams series<sup>71</sup>. These rules predict that the stability constants of transition-metal ion  
12 22 complexes increase by a factor of 100 to 1000 from Cd- towards Cu-thiolates<sup>72,73</sup>. However, The Irving  
13 23 Williams rules may not apply to metal-selective snail MTs, considering that they do not contain simple  
14 24 binary metal-thiolate complexes. In the CdMTs of *Littorina littorea* and *Helix pomatia*, for example,  
15 25 divalent Cd<sup>2+</sup> ions are tetrahedrally coordinated<sup>20,46</sup>, forming Cd-thiolate clusters that most likely differ  
16 26 in their structural configuration from the Cu-thiolate clusters of snail CuMTs<sup>14</sup>. Importantly, it was  
17 27 demonstrated that the replacement of a few amino acid positions in the near vicinity to the metal-  
18 28 coordinating Cys residues can have a strong impact on the metal binding preferences of snail MTs<sup>15,19,21</sup>,  
19 29 probably due to spatial and charge-dependent constraints upon formation of protein-metal complexes. We  
20 30 suspect that such amino acid replacements must have gradually improved/modified the Cd-binding  
21 31 selectivity of snail MTs during evolution. Apart from this, the capacity for Cd-loading of many snail  
22 32 CdMTs has been increased through evolutionary multiplication of Cd-binding domains as demonstrated  
23 33 for the littoral periwinkle, *Littorina littorea*, and the land snails *Pomatias elegans* and *Alinda biplicata*  
24 34<sup>16,20,47</sup>. At the functional level, evolutionary optimization for Cd binding in CdMTs has resulted in Cd-  
25 35 specific detoxification pathways within snail tissues. This is reflected by the fact that native purified  
26 36 gastropod CdMTs contain mainly Cd<sup>2+</sup>, but only small amounts of Zn<sup>2+</sup> or Cu<sup>+</sup> (**Figure 10A**).  
27 37 Concomitantly, Cd inactivation in these species is enhanced by metal-dependent upregulation of the  
28 38 respective *CdMT* genes (**Figure 10B**), and tissue or cell-specific expression of *CdMT* mRNA<sup>23,69,74</sup>.

## 50 341 6. Environmental Cd levels through the earth history: an important evolutionary driver

51 342 Cd is carcinogenic and highly toxic in animals, even at low concentrations<sup>75</sup>. The chemical  
52 343 similarity of this metal and its frequent co-occurrence with Zn in ore deposits of the earth crust make Cd  
53 344 a dangerous competitor for Zn-dependent cellular processes<sup>5</sup>. Cd can also compete with calcium (Ca)<sup>76</sup>,  
54 345 and hence affect gastropods that depend on Ca pathways for bio-mineralization of their shells<sup>77</sup>.

55 346 Gain of Cd-selective MTs may have provided an advantage particularly for gastropod lineages that  
56 347 have adapted to littoral, semi-terrestrial, and terrestrial conditions. Recent natural Cd concentrations in

seawater follow those of algal nutrients such as phosphate<sup>3</sup>, displaying higher concentrations in deeper oceanic waters and exhibit a depletion towards neritic surface waters down to concentrations of  $10^{-10}$  M<sup>78,79</sup> (**Figure 11**). Complex formation of Cd<sup>2+</sup> with inorganic and organic ligands further decreases its biological availability in neritic seawater realms<sup>80</sup>. The situation changes drastically in the littoral zone, where marine habitats come into contact with the continental earth crust, in which natural Cd background concentrations, at  $10^{-8}$  –  $10^{-7}$  M, can be up to 100 times higher than those of superficial seawater<sup>81</sup> (**Figure 11**). Decreasing seawater salinities in the supra-littoral zone can even enhance the availability of Cd<sup>2+</sup> for animals<sup>82,83</sup>.

Gastropods of these habitats have adapted to fluctuating environmental conditions<sup>84</sup> but also had to cope with increasing Cd concentrations. Inactivation of Cd<sup>2+</sup> ions by metal-selective MTs would, therefore, confer on them a physiological advantage<sup>85</sup> over energy-consuming activities for continuously re-adjusting intracellular Cd concentrations<sup>86</sup>. Upon adaptation to terrestrial life, gastropods have learned to cope with alternating and adverse environmental conditions<sup>87,88</sup>. Hence, the conservation of Cd-selective MTs may also be beneficial for land snails<sup>16</sup> (**Figure 11**).

In contrast to terrestrial snails, freshwater species of Caenogastropoda and Heterobranchia have lost their Cd binding selectivity, likely because natural Cd background concentrations in freshwater habitats with about  $10^{-10}$  –  $10^{-12}$  M are the lowest of any snail habitat on earth<sup>89</sup> (**Figure 11**).

The multitude of metal-selective MT variants naturally occurring in snails offers the unique possibility to apply them as models for optimization of MT metal binding features through experiments in the laboratory. This may promote our understanding of about how amino acid replacements modify metal selectivity in MTs, and could have implications for the design of novel artificial Cd-binding proteins for the sake of basic research or for application in environmental bioremediation<sup>90,91</sup>. It underscores once more the true model character of metal-selective snail MTs.

## 7. Conclusions

Some important conclusions are derived from our findings: First, presence of Cd has been a continuous evolutionary stimulus through the last 430 million years, driving convergent evolution and optimization of Cd-selective MTs in gastropod clades. Second, the C-terminal domain of Cd-selective gastropod MTs has been subjected to a high pressure for evolutionary conservation, which we attribute to its important role for immobilizing Cd<sup>2+</sup>. Third, gastropod adaptation to habitats with different Cd background levels has triggered MT diversification towards partial or complete loss of metal selectivity. Fourth, the natural evolution in snails of an array of differently metal-selective MT variants designates them MTs as model molecules and indicates that it is possible to design artificial Cd-selective peptides.

## Acknowledgements



1  
2 583 This work was funded by a cooperation grant to R.D. and O.Z. from the Austrian Science Fund  
3 and the Swiss National Science Foundation (DACH grant No I 1482-N28), and a grant from the  
4 584 View Article Online  
DOI: 10.1039/C9MT00059F  
5 585 Forschungskredit of the University of Zurich to C.B. (grant no. FK-18-083). B.E. was supported by a grant  
6 586 for young scientists at the University of Innsbruck. Researchers from Barcelona want to acknowledge the  
7 587 Spanish Ministerio de Ciencia e Innovación and FEDER for the projects BIO2015-67358-C2-2-P (M.C.  
8 and O.P.) and BIO2015-67358-C2-1-P (R.A.). M.C. and O.P. are members of the “Grup de Recerca de la  
9 588 Generalitat de Catalunya”, ref. 2017SGR-864.  
10  
11  
12  
13

14 590 We thank Thomas Ostermann for help with the transcriptome assembly and Philipp Andesner  
15 (both: University of Innsbruck, Austria) for producing the neutral marker sequences. Transcriptomic data  
16 591 have been achieved in part using the HPC infrastructure of the University of Innsbruck. We also thank the  
17 592 Servei d'Anàlisi Química (SAQ) at the Universitat Autònoma de Barcelona (ICP-AES, CD, UV-vis, ESI-  
18 593 MS) for allocating instrument time and three anonymous reviewers for constructive comments on an  
19 594 earlier version of the manuscript.  
20  
21  
22  
23  
24  
25  
26  
27  
28  
29  
30  
31  
32  
33  
34  
35  
36  
37  
38  
39  
40  
41  
42  
43  
44  
45  
46  
47  
48  
49  
50  
51  
52  
53  
54  
55  
56  
57  
58  
59  
60



## References

- 1 K. H. Wedepohl, *Geochim. Cosmochim. Acta*, 1995, **59**, 1217–1232.
- 2 J. T. Cullen and M. T. Maldonado, in *Cadmium: From Toxicity to Essentiality. Metal Ions in Life Sciences*, eds. A. Sigel, H. Sigel and R. Sigel, Springer, Dordrecht, 2013, pp. 31–62.
- 3 T. W. Lane and F. M. M. Morel, *Proc. Natl. Acad. Sci. U. S. A.*, 2000, **97**, 4627–4631.
- 4 T. W. Lane, M. A. Saito, G. N. George, I. J. Pickering, R. C. Prince and F. M. M. Morel, *Nature*, 2005, **434**, 42.
- 5 A. Martelli, E. Rousselet, C. Dycke, A. Bouron and J. M. Moulis, *Biochimie*, 2006, **88**, 1807–1814.
- 6 A. M. Sandbichler and M. Höckner, *Int. J. Mol. Sci.*, DOI:10.3390/ijms17010139.
- 7 C. D. Klaassen, J. Liu and S. Choudhuri, *Annu. Rev. Pharmacol. Toxicol.*, 1999, **39**, 267–294.
- 8 R. D. Palmiter, *Proc. Natl. Acad. Sci. U. S. A.*, 1998, **95**, 8428–8430.
- 9 S. G. Bell and B. L. Vallee, *ChemBioChem*, 2009, **10**, 55–62.
- 10 A. Krężel and W. Maret, *Int. J. Mol. Sci.*, 2017, **18**, 1237.
- 11 C. A. Blindauer and O. I. Leszczyszyn, *Nat. Prod. Rep.*, 2010, **27**, 720–741.
- 12 G. Isani and E. Carpenè, *Biomolecules*, 2014, **4**, 435–457.
- 13 S. Calatayud, M. Garcia-Risco, N. S. Rojas, L. Espinosa-Sánchez, S. Artime, O. Palacios, C. Cañestro and R. Albalat, *Metallomics*, 2018, **10**, 1585–1594.
- 14 R. Dallinger, B. Berger, P. Hunziker and J. H. R. Kägi, *Nature*, 1997, **388**, 237–238.
- 15 Ò. Palacios, A. Pagani, S. Pérez-Rafael, M. Egg, M. Höckner, A. Brandstätter, M. Capdevila, S. Atrian and R. Dallinger, *BMC Biol.*, DOI:10.1186/1741-7007-9-4.
- 16 L. Schmielau, M. Dvorak, M. Niederwanger, N. Dobieszewski, V. Pedrini-Martha, P. Ladurner, J. Rodríguez-Guerra Pedregal, J. D. Maréchal and R. Dallinger, *Sci. Total Environ.*, 2019, **648**, 561–571.
- 17 S. Pérez-Rafael, A. Mezger, B. Lieb, R. Dallinger, M. Capdevila, Ò. Palacios and S. Atrian, *J. Inorg. Biochem.*, 2012, **108**, 84–90.
- 18 Ò. Palacios, S. Pérez-Rafael, A. Pagani, R. Dallinger, S. Atrian and M. Capdevila, *J. Biol. Inorg. Chem.*, 2014, **19**, 923–935.
- 19 S. Pérez-Rafael, F. Monteiro, R. Dallinger, S. Atrian, Ò. Palacios and M. Capdevila, *Biochim. Biophys. Acta - Proteins Proteomics*, 2014, **1844**, 1694–1707.
- 20 C. Baumann, A. Beil, S. Jurt, M. Niederwanger, O. Palacios, M. Capdevila, S. Atrian, R. Dallinger and O. Zerbe, *Angew. Chemie - Int. Ed.*, 2017, **56**, 4617–4622.
- 21 M. Niederwanger, S. Calatayud, O. Zerbe, S. Atrian, R. Albalat, M. Capdevila, Ò. Palacios and R. Dallinger, *Int. J. Mol. Sci.*, DOI:10.3390/ijms18071457.
- 22 Ò. Palacios, E. Jiménez-Martí, M. Niederwanger, S. Gil-Moreno, O. Zerbe, S. Atrian, R. Dallinger and M. Capdevila, *Int. J. Mol. Sci.*, 2017, **18**, 1–16.
- 23 M. Dvorak, R. Lackner, M. Niederwanger, C. Rotondo, R. Schnegg, P. Ladurner, V. Pedrini-Martha, W. Salvenmoser, L. Kremser, H. Lindner, M. Garcia-Risco, S. Calatayud, R. Albalat, Ò. Palacios, M. Capdevila and R. Dallinger, *Metallomics*, 2018, **10**, 1638–1654.
- 24 R. Dallinger, M. Chabicovsky and B. Berger, *Environ. Toxicol. Chem.*, 2004, **23**, 890–901.
- 25 K. M. Jörger, I. Stöger, Y. Kano, H. Fukuda, T. Kneblsberger and M. Schrödl, *BMC Evol. Biol.*, DOI:10.1186/1471-2148-10-323.
- 26 M. Höckner, K. Stefanon, D. Schuler, R. Fantur, A. De Vaufleury and R. Dallinger, *J. Exp. Zool. Part A Ecol. Genet. Physiol.*, 2009, **311**, 776–787.
- 27 M. G. Grabherr, B. J. Haas, M. Yassour, J. Z. Levin, D. A. Thompson, I. Amit, X. Adiconis, L. Fan, R. Raychowdhury, Q. Zeng, Z. Chen, E. Mauceli, N. Hacohen, A. Gnirke, N. Rhind, F. Di Palma, B. W. Birren, C. Nusbaum, K. Lindblad-Toh, N. Friedman and A. Regev, *Nat. Biotechnol.*, 2011, **29**, 644–652.
- 28 A. Priyam, B. J. Woodcroft, V. Rai, A. Munagala, I. Moghul, F. Ter, M. A. Gibbins, H. Moon, G. Leonard, W. Rumpf and Y. Wurm, *BioRxiv*, 2015, 033142.
- 29 V. Pedrini-Martha, M. Niederwanger, R. Kopp, R. Schnegg and R. Dallinger, *PLoS One*, 2016, **11**, 1–19.
- 30 R. C. Edgar, *Nucleic Acids Res.*, 2004, **32**, 1792–7.
- 31 A. Stamatakis, *Bioinformatics*, 2014, **30**, 1312–1313.
- 32 F. Ronquist, M. Teslenko, P. Van Der Mark, D. L. Ayres, A. Darling, S. Höhna, B. Larget, L. Liu, M. A. Suchard and J. P. Huelsenbeck, *Syst. Biol.*, 2012, **61**, 539–542.
- 33 E. Pruesse, J. Peplies and F. O. Glöckner, *Bioinformatics*, 2012, **28**, 1823–1829.
- 34 J. Trifinopoulos, L. T. Nguyen, A. von Haeseler and B. Q. Minh, *Nucleic Acids Res.*, 2016, **44**, W232–W235.
- 35 D. Posada and K. A. Crandall, *Bioinformatics*, 1998, **14**, 817–818.
- 36 P. Schanda, E. Kupce and B. Brutscher, *J. Biomol. NMR*, 2005, **33**, 199–211.
- 37 W. F. Vranken, W. Boucher, T. J. Stevens, R. H. Fogh, A. Pajon, M. Llinas, E. L. Ulrich, J. L. Markley, J. Ionides and E. D. Laue, *Proteins Struct. Funct. Bioinforma.*, 2005, **59**, 687–696.
- 38 S. Meiboom and D. Gill, *Rev. Sci. Instrum.*, 1958, **29**, 688–691.
- 39 A. Dinapoli and A. Klussmann-Kolb, *Mol. Phylogenet. Evol.*, 2010, **55**, 60–76.
- 40 B. Dayrat, M. Conrad, S. Balayan, T. R. White, C. Albrecht, R. Golding, S. R. Gomes, M. G. Harasewych and A. M. de Frias Martins, *Mol. Phylogenet. Evol.*, 2011, **59**, 425–437.

- 1  
2660 41 F. Zapata, N. G. Wilson, M. Howison, S. C. S. Andrade, K. M. Jörger, M. Schrödl, F. E. Goetz, G. Giribet and C. W.  
3661 Dunn, *Proc. R. Soc. B*, 2014, **281**, 20141739.
- 4662 42 O. Razkin, B. J. Gómez-Moliner, C. E. Prieto, A. Martínez-Ortí, J. R. Arrébola, B. Muñoz, L. J. Chuca and M. J.  
5663 Madeira, *Mol. Phylogenet. Evol.*, 2015, **83**, 99–117.
- 6664 43 T. J. Cunha and G. Giribet, *Proc. R. Soc. B Biol. Sci.*, 2019, **286**, 20182776.
- 7665 44 H. Yang, J. Zhang, J. Xia, J. Yang, J. Guo, Z. Deng and M. Luo, *Int. J. Mol. Sci.*, 2018, **19**, 3646.
- 8666 45 A. Klussmann-Kolb, A. Dinapoli, K. Kuhn, B. Streit and C. Albrecht, *BMC Evol. Biol.*, DOI:10.1186/1471-2148-8-  
9667 57.
- 10668 46 A. Beil, S. Jurt, R. Walser, T. Schönhut, P. Güntert, Ò. Palacios, S. Atrian, M. Capdevila, R. Dallinger and O. Zerbe,  
11669 *Biochemistry*, 2019, **58**, 4570–4581.
- 12670 47 V. Pedrini-Martha, S. Köll, M. Dvorak and R. Dallinger, *Int. J. Mol. Sci.*, 2020, submitted.
- 13671 48 R. Orihuela, J. Domènech, R. Bofill, C. You, E. A. Mackay, J. H. R. Kägi, M. Capdevila and S. Atrian, *J. Biol. Inorg.*  
14672 *Chem.*, 2008, **13**, 801–812.
- 15673 49 N. Romero-Isart and M. Vašák, *J. Inorg. Biochem.*, 2002, **88**, 388–396.
- 16674 50 Kägi J.H.R., in *Metallothionein III: Biological Roles and Medical Implications, Proceedings of the Metallothionein*  
17675 *International Conference, 1992, Tsukuba, Japan*, Birkhauser Verlag, Boston, 1993, vol. 3, pp. 29–56.
- 18676 51 E. H. Fischer and E. W. Davie, *Proc. Natl. Acad. Sci. U. S. A.*, 1998, **95**, 3333–3334.
- 19677 52 P. M. Gehrig, C. You, R. Dallinger, C. Gruber, M. Brouwer, J. H. R. Kägi and P. E. Hunziker, *Protein Sci.*, 2000, **9**,  
20678 395–402.
- 21679 53 K. M. Kocot, K. M. Halanych and P. J. Krug, *Mol. Phylogenet. Evol.*, 2013, **69**, 764–771.
- 22680 54 R. Dallinger, M. Chabicoovsky, E. Hödl, C. Prem, P. Hunziker and C. Manzl, *Am. J. Physiol. Integr. Comp. Physiol.*,  
23681 2005, **289**, R1185–R1195.
- 24682 55 M. Höckner, K. Stefanon, A. De Vaufleury, F. Monteiro, S. Pérez-Rafael, Ò. Palacios, M. Capdevila, S. Atrian and  
25683 R. Dallinger, *Biometals*, 2011, **24**, 1079–1092.
- 26684 56 E. B. Naimark and A. V. Markov, *Biol. Bull. Rev.*, 2011, **1**, 71–81.
- 27685 57 S. E. Grasby, B. Beauchamp, D. P. G. Bond, P. Wignall, C. Talavera, J. M. Galloway, K. Piepjohn, L. Reinhardt and  
28686 D. Blomeier, *Bull. Geol. Soc. Am.*, 2015, **127**, 1331–1347.
- 29687 58 D. P. G. Bond and S. E. Grasby, *Palaeogeogr. Palaeoclimatol. Palaeoecol.*, 2017, **478**, 3–29.
- 30688 59 G. Keller, P. Mateo, J. Punekar, H. Khozyem, B. Gertsch, J. Spangenberg, A. M. Bitchong and T. Adatte, *Gondwana*  
31689 *Res.*, 2018, **56**, 69–89.
- 32690 60 S. Aizawa and H. Akaiwa, *Chem. Geol.*, 1992, **98**, 103–110.
- 33691 E. Porębska and Z. Sawłowicz, *Palaeogeogr. Palaeoclimatol. Palaeoecol.*, 1997, **132**, 343–354.
- 34692 62 M. L. W. Tuttle, G. N. Breit and M. B. Goldhaber, *Appl. Geochemistry*, 2009, **24**, 1565–1578.
- 35693 63 Y. Liu, T. Xiao, R. B. Perkins, J. Zhu, Z. Zhu, Y. Xiong and Z. Ning, *J. Geochemical Explor.*, 2017, **176**, 42–49.
- 36694 64 H. J. Brumsack, *Palaeogeogr. Palaeoclimatol. Palaeoecol.*, 2006, **232**, 344–361.
- 37695 65 F. Batifol, C. Boutron and M. De Angelis, *Nature*, 1989, **337**, 544–546.
- 38696 66 V. Pedrini-Martha, R. Schnegg, P. E. Baurand, A. deVaufleury and R. Dallinger, *Comp. Biochem. Physiol. Part - C*  
39697 *Toxicol. Pharmacol.*, 2017, **199**, 38–47.
- 40698 67 P. E. Baurand, V. Pedrini-Martha, A. De Vaufleury, M. Niederwanger, N. Capelli, R. Scheifler and R. Dallinger,  
41699 *PLoS One*, 2015, **10**, 1–14.
- 42700 68 P. E. Baurand, R. Dallinger, M. Niederwanger, N. Capelli, V. Pedrini-Martha and A. de Vaufleury, *Environ. Sci.*  
43701 *Pollut. Res.*, 2016, **23**, 3062–3067.
- 44702 69 M. Chabicoovsky, H. Niederstätter, R. Thaler, E. Hödl, W. Parson, W. Rossmanith and R. Dallinger, *Toxicol. Appl.*  
45703 *Pharmacol.*, 2003, **190**, 25–36.
- 46704 70 F. Hispard, D. Schuler, A. De Vaufleury, R. Scheifler, P. M. Badot and R. Dallinger, *Environ. Toxicol. Chem.*, 2008,  
47705 **27**, 1533–1542.
- 48706 71 H. Irving and R. J. P. Williams, *J. Chem. Soc.*, 1953, 3192–3210.
- 49707 72 M. Erk and B. Raspor, *Anal. Chim. Acta*, 1998, **360**, 189–194.
- 50708 73 G. Meloni, V. Sonois, T. Delaine, L. Guilloreau, A. Gillet, J. Teissie, P. Faller and M. Vasak, *Nat. Chem. Biol.*, 2008,  
51709 **4**, 366–372.
- 52710 74 E. Hödl, E. Felder, M. Chabicoovsky and R. Dallinger, *Cell Tissue Res.*, 2010, **341**, 159–171.
- 53711 75 W. Maret and J. M. Moulis, in *Cadmium: From Toxicity to Essentiality. Metal Ions in Life Sciences*, eds. A. Sigel, H.  
54712 Sigel and R. Sigel, Springer, Dordrecht, 2013, pp. 1–29.
- 55713 76 G. Choong, Y. Liu and D. M. Templeton, *Chem. Biol. Interact.*, 2014, **211**, 54–65.
- 56714 77 D. Faubel, M. Lopes-Lima, S. Freitas, L. Pereira, J. Andrade, A. Checa, H. Frank, T. Matsuda and J. Machado, *Mar.*  
57715 *Freshw. Behav. Physiol.*, 2008, **41**, 93–108.
- 58716 78 E. A. Boyle, F. Sclater and J. M. Edmond, *Nature*, 1976, **263**, 42–44.
- 59717 79 W. Abouchami, S. J. G. Galer, H. J. W. De Baar, R. Middag, D. Vance, Y. Zhao, M. Klunder, K. Mezger, H.  
60718 Feldmann and M. O. Andreae, *Geochim. Cosmochim. Acta*, 2014, **127**, 348–367.
- 61719 80 K. W. Bruland, *Limnol. Oceanogr.*, 1992, **37**, 1008–1017.
- 62720 81 S. Sposito, in *Metal Ions in Biological Systems, Vol. 20, Concepts on Metal Ion Toxicity*, eds. H. Sigel and A. Sigel,  
63721 Marcel Dekker Inc., New York, 1986, pp. 1–20.

- 1  
2722 82 P. Bjerregaard and M. H. Depledge, *Mar. Biol.*, 1994, **119**, 385–395.  
3723 83 G. Roesijadi, *Mar. Environ. Res.*, 1994, **38**, 147–168.  
4724 84 K. B. Storey, B. Lant, O. O. Anozie and J. M. Storey, *Comp. Biochem. Physiol. Part A*, 2013, **165**, 448–459.  
5725 85 T. E. English and K. B. Storey, *J. Exp. Biol.*, 2003, **206**, 2517–2524.  
6726 86 M. H. Depledge and P. S. Rainbow, *Comp. Biochem. Physiol.*, 1990, **97C**, 1–7.  
7727 87 S. Slotsbo, K. V. Fisker, L. M. Hansen and M. Holmstrup, *J. Comp. Physiol. B*, 2011, **181**, 1001–1009.  
8728 88 T. Bishop and M. D. Brand, *J. Exp. Biol.*, 2000, **203**, 3603–12.  
9729 89 C. A. Mebane, in *US Department of the Interior & US Geological Survey*, Scientific Investigations Report 2006-5245, Reston, Virginia, v. 1.2., 2010, p. 130.  
10730  
11731 90 A. F. A. Peacock and V. L. Pecoraro, in *Cadmium: From Toxicity to Essentiality (Metal Ions in Life Sciences Vol. 11)*, eds. A. Sigel, H. Sigel and R. Sigel, Springer, Dordrecht, 2013, pp. 303–338.  
12732  
13733 91 M. Mejáre and L. Bülow, *Trends Biotechnol.*, 2001, **19**, 67–73.  
14734 92 K. M. Kocot, J. T. Cannon, C. Todt, M. R. Citarella, A. B. Kohn, A. Meyer, S. R. Santos, C. Schander, L. L. Moroz, B. Lieb and K. M. Halanych, *Nature*, 2011, **477**, 452–456.  
15735  
16736 93 D. J. Colgan, W. F. Ponder, E. Beacham and J. Macaranas, *Mol. Phylogenet. Evol.*, 2007, **42**, 717–737.  
17737 94 C. M. Wade, P. B. Mordan and B. Clarke, *Proc. R. Soc. B*, 2001, **268**, 413–422.  
18738 95 E. V. Soldatenko and A. A. Petrov, *J. Morphol.*, 2019, **280**, 508–525.  
19739 96 M. Niederwanger, M. Dvorak, R. Schnegg, V. Pedrini-Martha, K. Bacher, M. Bidoli and R. Dallinger, *Int. J. Mol. Sci.*, 2017, **18**, 1747.  
20740  
21741 97 D. Benito, M. Niederwanger, U. Izagirre, R. Dallinger and M. Soto, *Int. J. Mol. Sci.*, 2017, **18**, 1815.  
22742  
23743  
24744  
25745  
26746  
27747  
28748  
29749  
30750  
31751  
32752  
33753  
34754  
35755  
36  
37  
38  
39  
40  
41  
42  
43  
44  
45  
46  
47  
48  
49  
50  
51  
52  
53  
54  
55  
56  
57  
58  
59  
60

View Article Online  
DOI: 10.3390/C9MT00259F



### Figure 1A-E: Sequence alignments of snail metallothioneins.

Cys positions are underlaid in pink, conserved non-Cys positions through sequences of both clades are underlaid in light blue. Identical amino acid positions between pairwise aligned sequences are indicated by black stars. Domain boundaries of the N-terminal and the C-terminal domain (designated above the alignments with N and C) are indicated by bold red lines. The linker between the two domains is shown in black letters, its boundary is symbolized by a dotted line. The gaps between the two domains were inserted indicating the lack of a second N-terminal domain (present in other gastropod MTs). MTs of species shown in red letters were sequenced in this study for the first time while sequences in black letters were downloaded from publications or databases. Species for which metal selectivity features of respective MTs were documented experimentally by us through MS or NMR methods elsewhere are framed in blue.

A

#### VETIGASTROPODA

*Megathura crenuata* MT

*Haliotis diversicolor* MT

*Haliotis discus hanai* MT

*Haliotis tuberculata* MT

*Haliotis laevigata* MT

*Tegula atra* MT

#### NERITIMORPHA

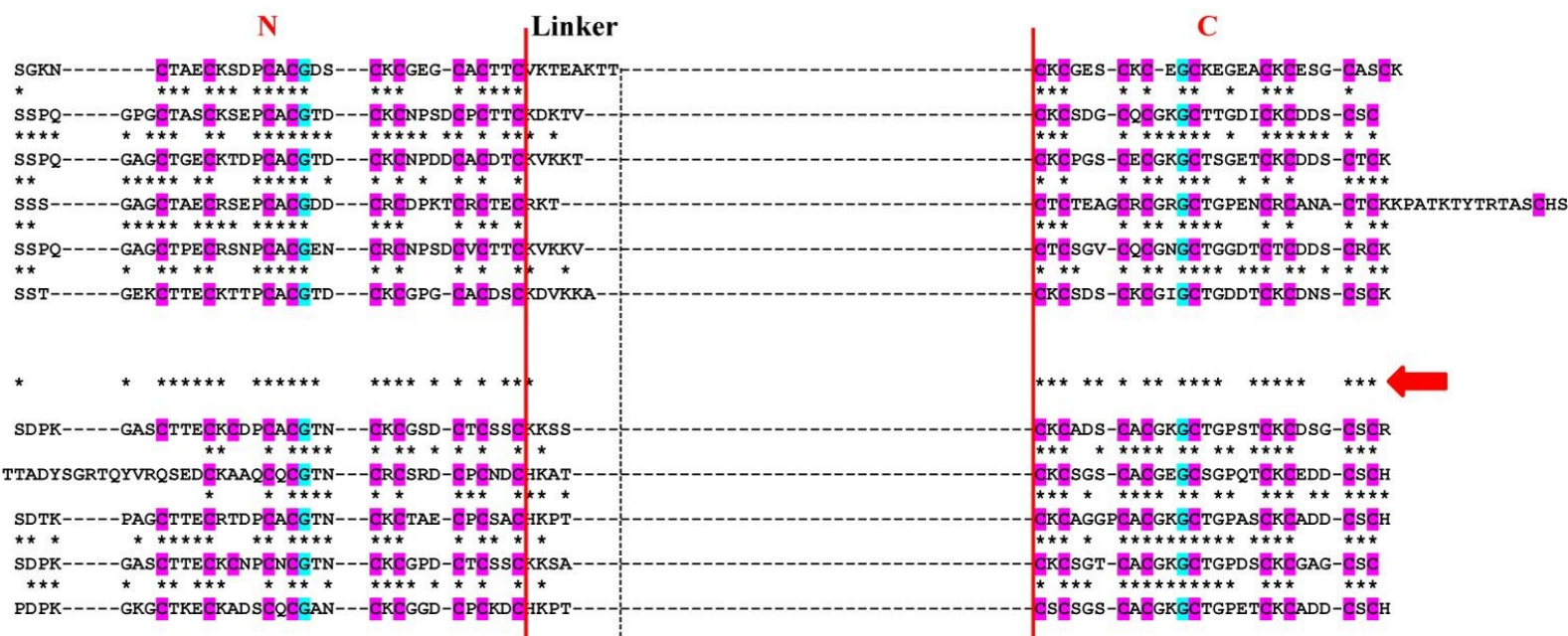
*Neritina peloronta* MT1

*Neritina peloronta* MT2

*Titiscania limacina* MT1

*Neritina pulligera* MT1

*Neritina pulligera* MT2



Metal-binding domain organization and amino acid sequence alignment of unspecific MTs from the gastropod clade of Vetigastropoda and MTs with still unknown metal binding features from Neritimorpha. The bold red arrow on the right hand of the alignments points to sequence identities between MTs of *Tegula atra* (Vetigastropoda) and *Neritina peloronta* MT1 (Neritimorpha).

**PATELLOGASTROPODA**

*Lottia gigantea* MT1

*Lottia gigantea* MT2

*Nacella polaris* MT

*Patella vulgata* MT1

*Patella vulgata* MT2

**CAENOCASTROPODA (Littorinoidea)**

*Littorina littorea* MT

*Pomatias elegans* MT1

*Pomatias elegans* MT2

**HETEROBRANCHIA (Stylommatophora)**

*Helix pomatia* CdMT

*Cornu aspersum* CdMT

*Arianta arbustorum* CdMT

*Cepaea hortensis* CdMT1

*Cepaea hortensis* CdMT2

*Cepaea nemoralis* CdMT

*Cochlicella acuta* CdMT

*Nesiohelix samarangae* CdMT

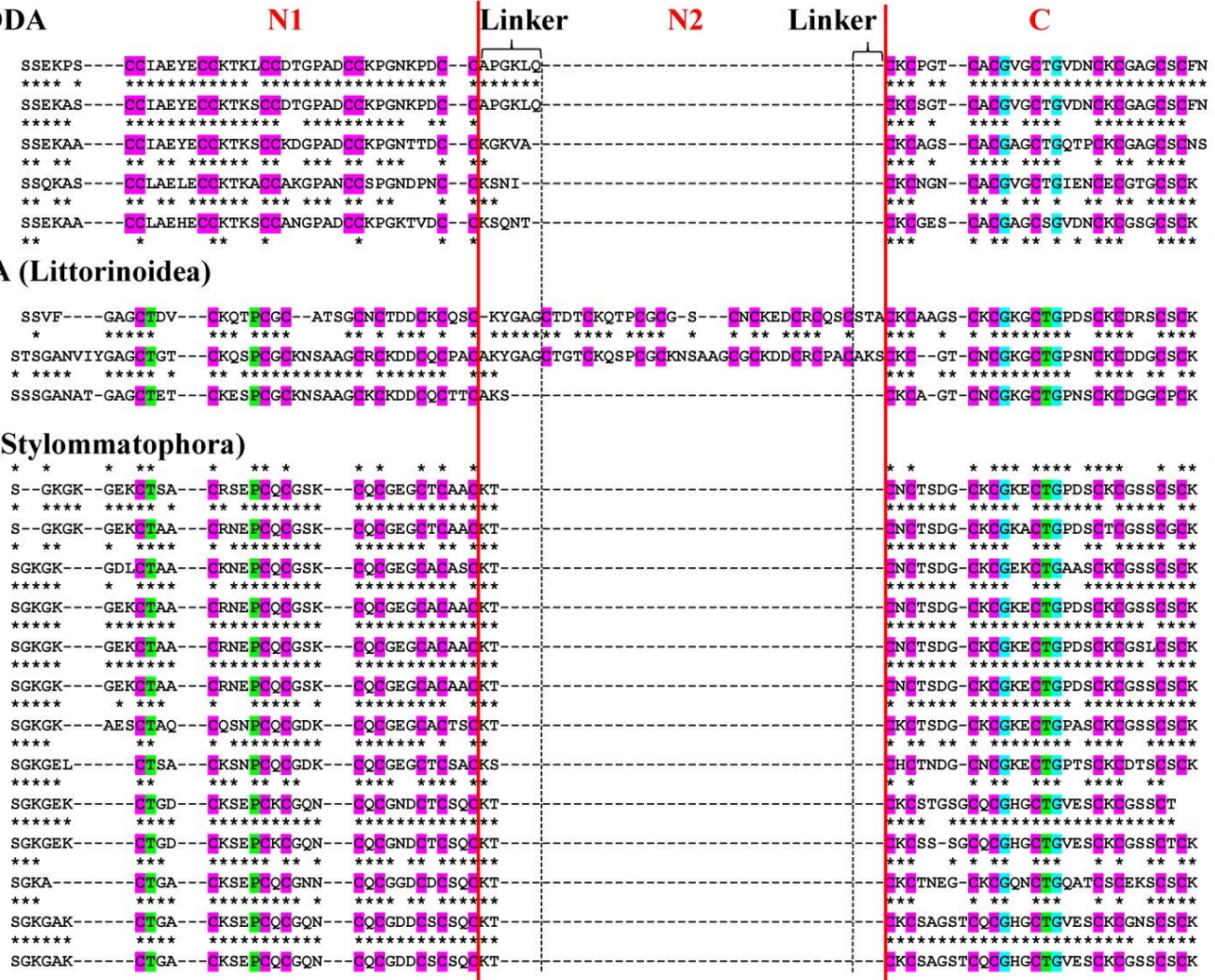
*Deroceras reticulatum* CdMT1

*Deroceras reticulatum* CdMT2

*Arion vulgaris* AvMT1

*Lehmannia nyctelia* CdMT

*Limax maximus* CdMT



**B** Metal-binding domain organization and amino acid sequence alignment of Cd-selective MTs from the gastropod clades of Patellogastropoda, Caenogastropoda and Heterobranchia using the same annotations as described in Figure 1A. The bold red arrows on the right hand of the alignments points to sequence differences or similarities between MTs of the three clades.

Published on 10 March 2020. Downloaded by Umeå University on 3/10/2020 11:11







859  
860  
861  
862  
863  
864  
865  
866  
867  
868  
869  
870  
871  
872  
873  
874  
875  
876  
877  
878  
879  
880  
881  
882  
883  
884  
885  
886  
887  
888  
889  
890  
891  
892  
893  
894  
895  
896  
897  
898  
899  
900  
901  
902  
903  
904  
905  
906  
907  
908  
909  
910  
911  
912  
913  
914  
915  
916  
917  
918  
919  
920  
921  
922  
923  
924  
925  
926  
927  
928  
929  
930  
931  
932  
933  
934  
935  
936  
937  
938  
939  
940  
941  
942  
943  
944  
945  
946

**Calyptraeidae**

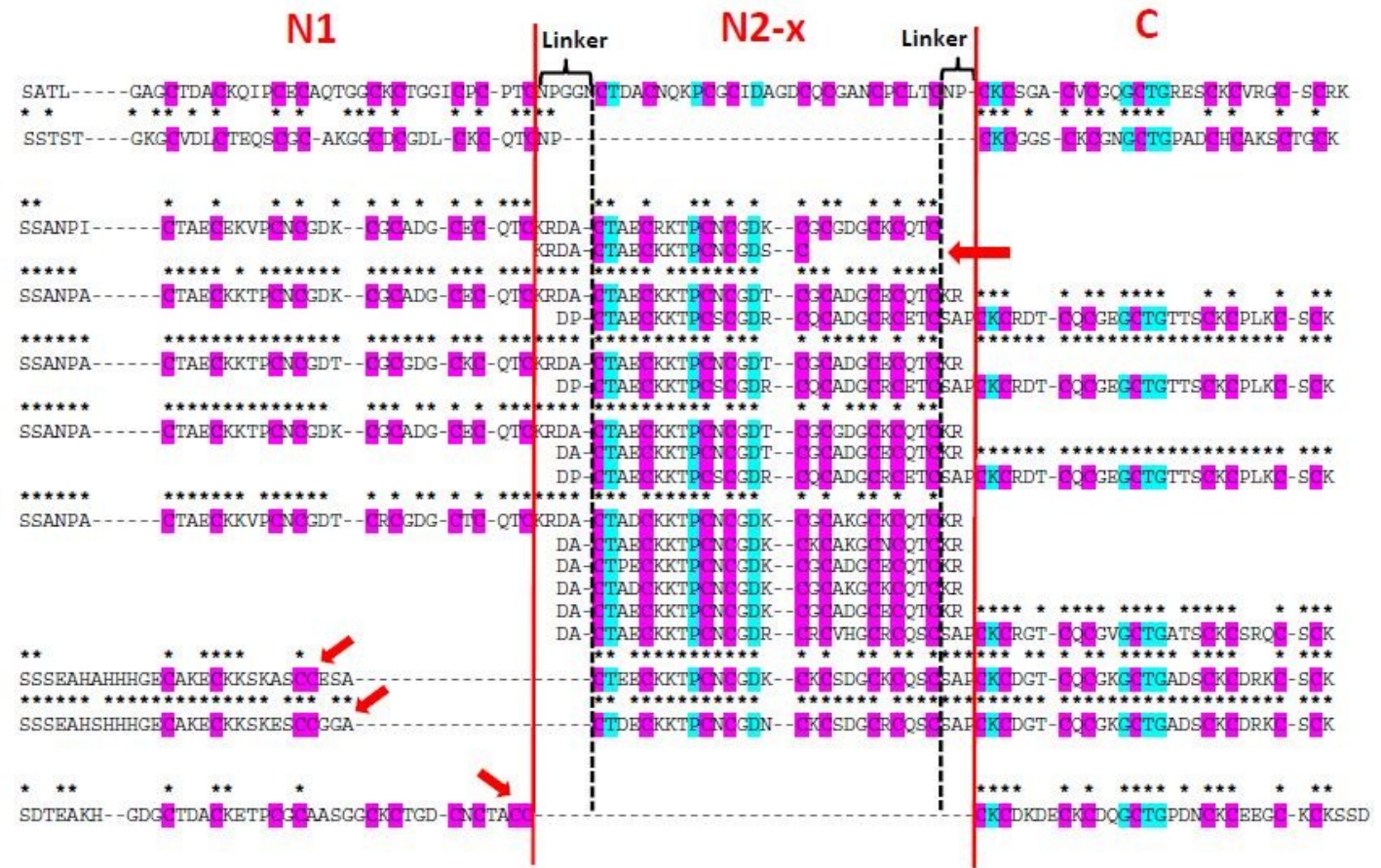
*Crepidula fornicata* MTa  
*Bostrycapulus* sp. MT

**Ampullariidae**

*Pomacea bridgesii* MT2  
*Pomacea canaliculata* MT1  
*Pomacea canaliculata* MT2  
*Pomacea canaliculata* MT3  
*Marisa cornuarietis* 8mg-MT  
*Pomacea bridgesii* MT1  
*Marisa cornuarietis* MT1

**Buccinidae**

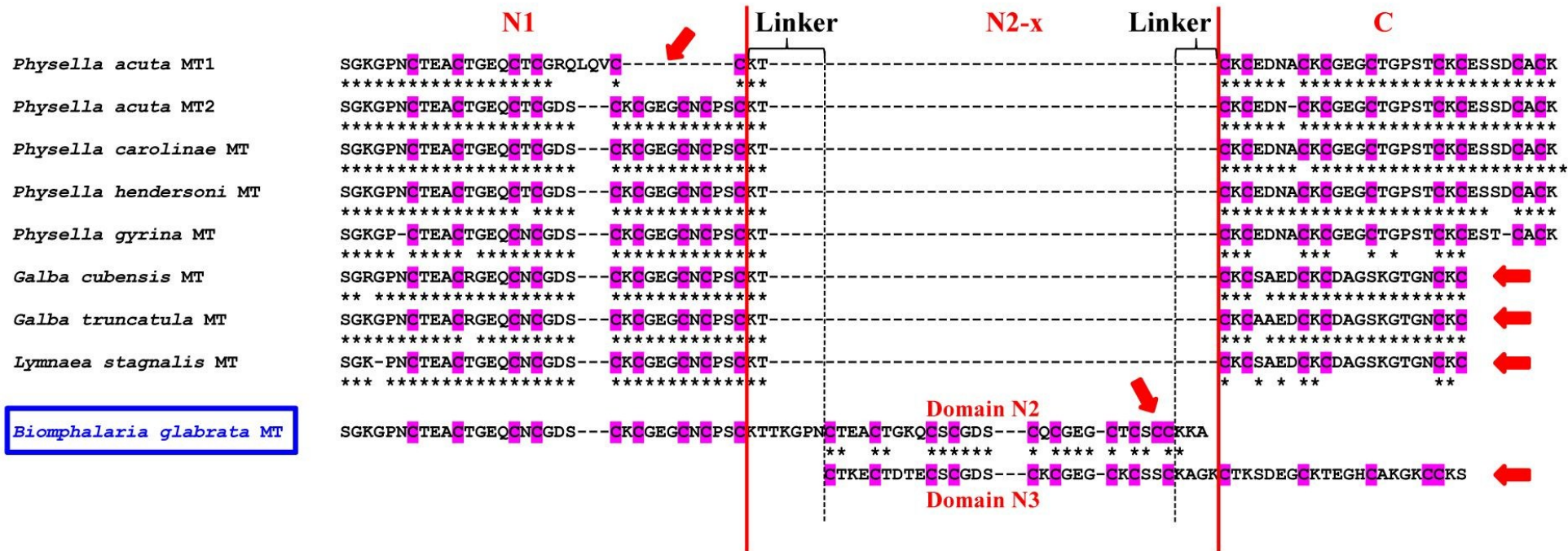
*Anentome helena* MT



**D** Metal-binding domain organization and amino acid sequence alignment of two and multi-domain MTs from freshwater families (with Calyptraeidae, Ampullariidae and Buccinidae) of the clade of Caenogastropoda. The bold red arrows above or besides some sequences point to sequence irregularities such as truncations or Cys replacements.

Metallomics Accepted Manuscript

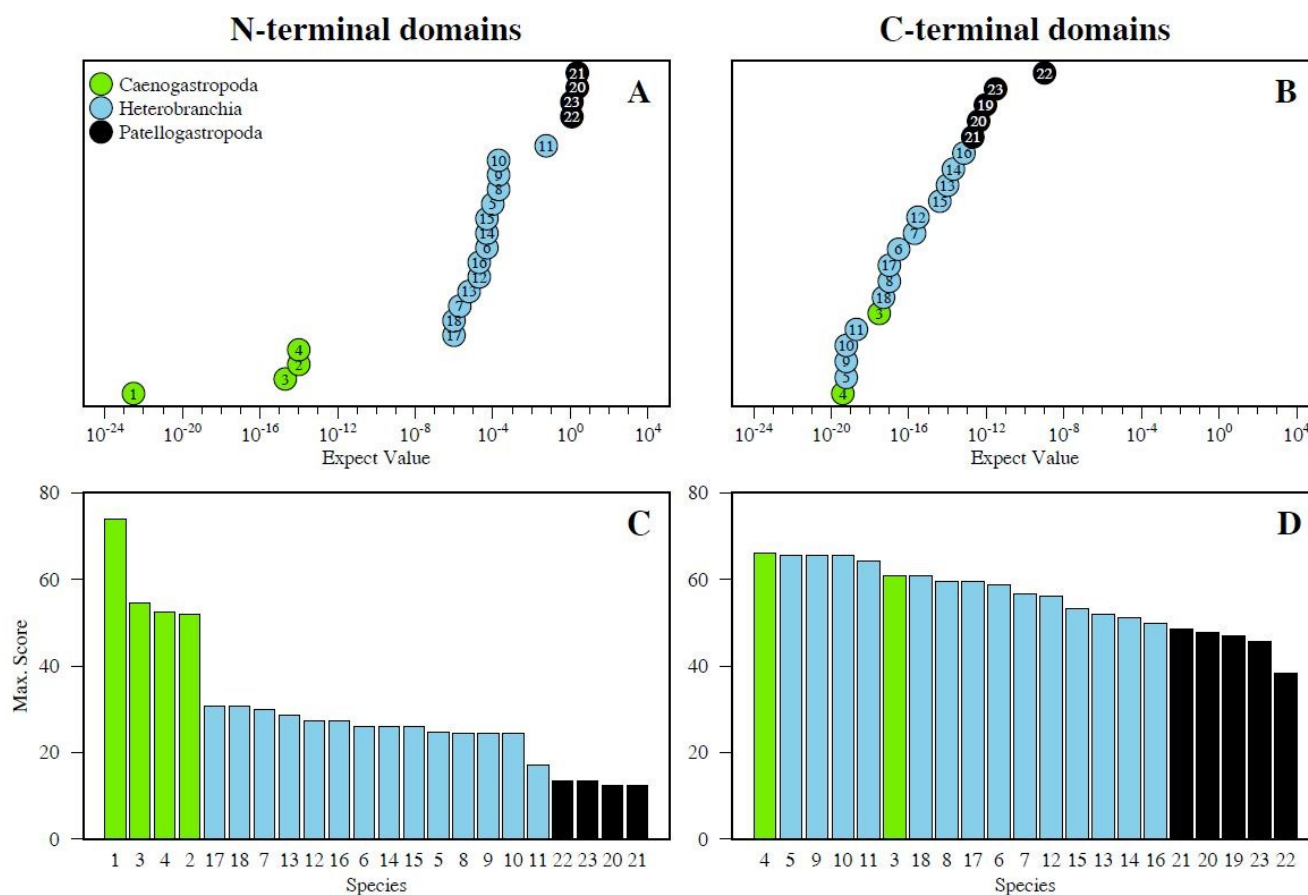
Hygrophila



**E** Metal-binding domain organization and amino acid sequence alignment of unspecific two and multi-domain MTs from the freshwater snail order of Hygrophila of the clade of Heterobranchia. N and C-terminal domains are designated in red letters above the alignments by N1, N2-x and C, and as Domain N2 and Domain N3 for *Biomphalaria glabrata*. The bold red arrows above or besides some sequences point to sequence irregularities such as gaps, truncations or Cys replacements.

927

View Article Online  
DOI: 10.1039/C9MT00259F



928

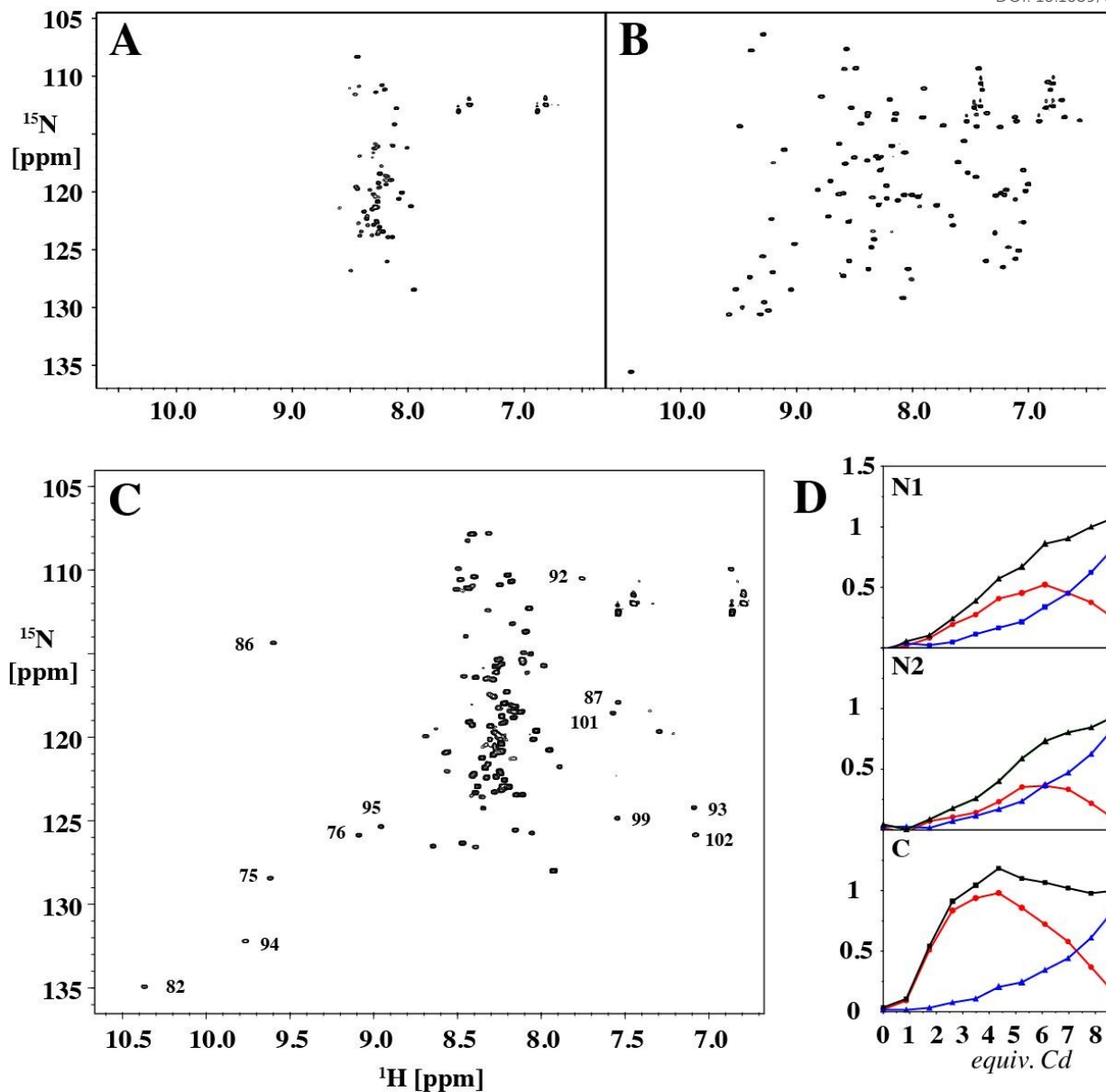
929 **Figure 2: Conservation between N- and C-terminal domains in CdMTs of Caenogastropoda (green**  
 930 **symbols or bars), Heterobranchia (blue symbols or bars) and Patellogastropoda (black**  
 931 **bars).** Shown are Expect Values in ascending order (A, B) and Homology Scores in descending order  
 932 (C, D), calculated with BLASTp. N-terminal domains (A, C) and C-terminal domains (B, D) of Cd-  
 933 selective MTs were compared to the N-terminal (N1-domain) and to the C-terminal domain of *Littorina*  
 934 *littorea* MT. N-terminal domains are less conserved through evolution (higher differences in e-values and  
 935 scores) than the C-terminal domains.

936 **Species labels:** 1, *Littorina littorea* MT (N2-domain); 2, *Pomatias elegans* MT1 (N1-domain); 3,  
 937 *Pomatias elegans* MT1 (N2- & C-domain); 4, *Pomatias elegans* MT2; 5, *Helix pomatia* CdMT; 6, *Cornu*  
 938 *aspersum* CdMT; 7, *Arianta arbustorum* CdMT; 8, *Cepaea hortensis* CdMT1; 9, *Cepaea hortensis*  
 939 CdMT2; 10, *Cepaea nemoralis* CdMT; 11, *Cochlicella acuta* CdMT; 12, *Nesiohelix samarangae* CdMT;  
 940 13, *Alinda biplicata* CdMT; 14, *Deroceras reticulatum* CdMT1 15, *Deroceras reticulatum* CdMT2; 16,  
 941 *Arion vulgaris* AvMT1; 17, *Lehmannia nyctelia* CdMT; 18, *Limax maximus* CdMT; 19, *Lottia gigantea*  
 942 MT1; 20, *Lottia gigantea* MT2; 21, *Nacella polaris* MT; 22, *Patella vulgata* MT1; 23, *Patella vulgata*  
 943 MT2.

944

945



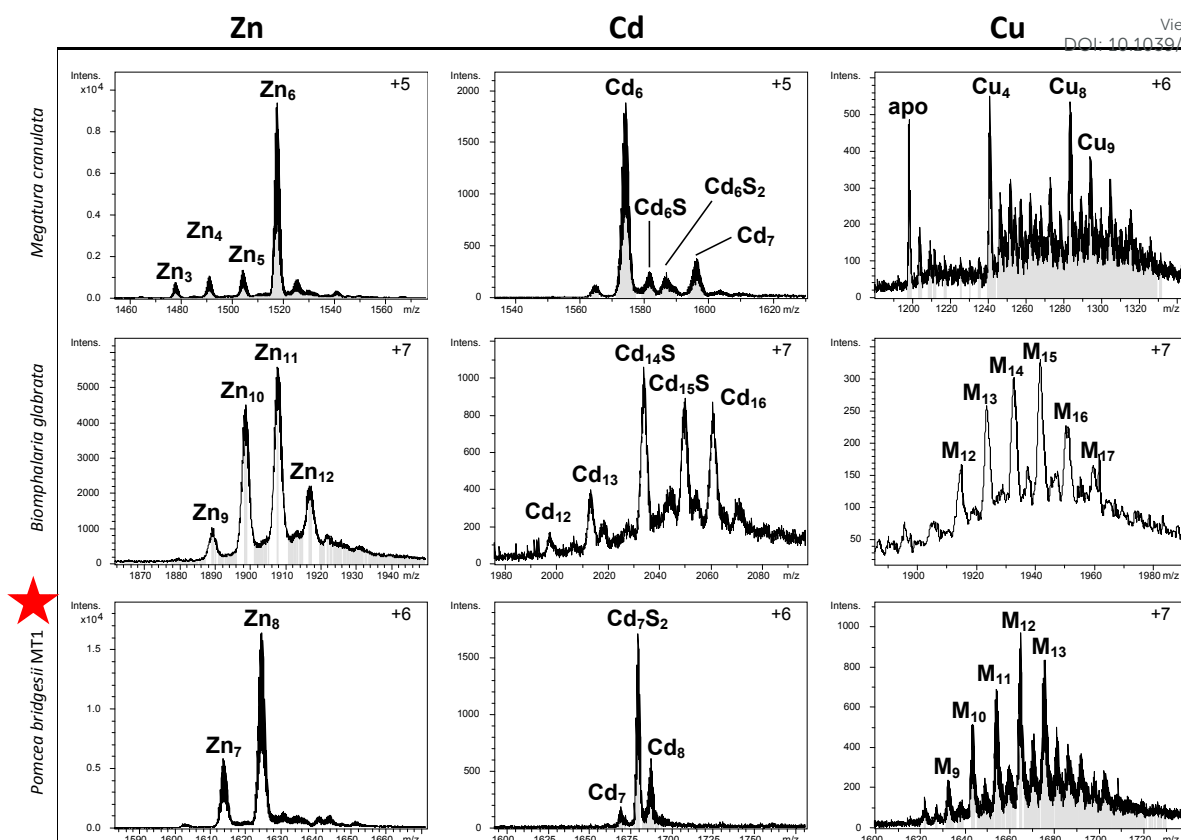


947

948 **Figure 3: Metallation of apo-MT from *Littorina littorea* (LIMT) with  $\text{Cd}^{2+}$ .**  $^{15}\text{N}$ ,  $^1\text{H}$ -HSQC spectrum  
 949 of apo (A) and fully-metallated (B) ( $\text{Cd}_9$ )-LIMT. C  $^{15}\text{N}$ ,  $^1\text{H}$ -HSQC spectrum after addition of 2 equiv.  
 950 of  $\text{Cd}^{2+}$  to apo-LIMT. Peaks close to positions in the fully-metallated form are annotated, and exclusively  
 951 stem from the metallated C-terminal domain. D Normalized average relative peak volumes of peaks from  
 952 the first (top) and second (center) N-terminal as well as the C-terminal (bottom) domains. Mostly, two  
 953 peaks are observed for each residue corresponding to apo (red) and metallated (blue) neighboring domains  
 954 (in the case of peaks from the C-terminal domain that corresponds to species in which the N2 domain is  
 955 already metallated). The black line corresponds to the sum intensity of both peaks.

956

957



958

959

960

961

962

963

964

965

966

967

968

969

970

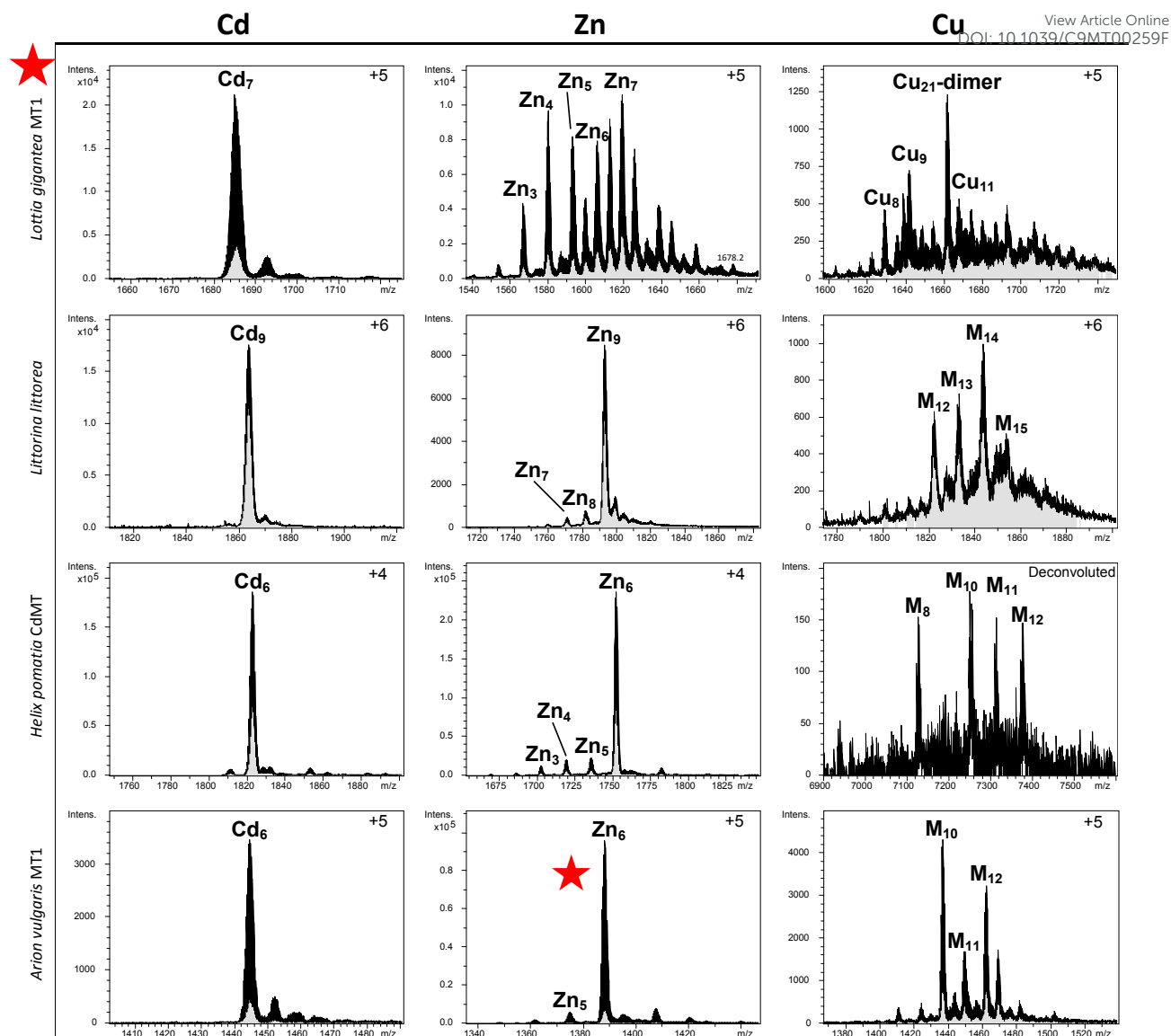
971

972

**Figure 4: ESI-MS spectra of metal-unselective gastropod MTs recombinantly produced in media containing Cd, Zn and Cu ions.** Data are shown for MTs from *Megathura crenulata* (Vetigastropoda), *Biomphalaria glabrata* (freshwater Heterobranchia) and *Pomacea bridgesii* (freshwater Caenogastropoda). The corresponding charge state is indicated in the upper right corner. In Cu productions, M denotes mixtures of Zn+Cu. Spectra of *pomacea bridgesii* MT1 are shown here for the first time and are marked with a red star. Spectra of other MTs are re-drawn from data reported in <sup>17,21</sup>.

Metallomics Accepted Manuscript

973



974

975 **Figure 5: ESI-MS spectra of Cd-selective gastropod MTs recombiantly produced in media**  
 976 **containing Cd, Zn and Cu ions. Data are shown for MTs from *Lottia gigantea* (Patellogastropoda),**  
 977 ***Littorina littorea* (Caenogastropoda), *Helix pomatia* (terrestrial snail, Heterobranchia) and *Arion vulgaris***  
 978 **(terrestrial slug, Heterobranchia). The corresponding charge state is indicated in the upper right corner.**  
 979 **In Cu productions, M denotes mixtures of Zn+Cu. Spectra for which metal selectivity features are shown**  
 980 **here for the first time are marked with a red star. Spectra of other MTs are re-drawn from data reported**  
 981 **in <sup>22,15,23</sup>.**  
 982



983

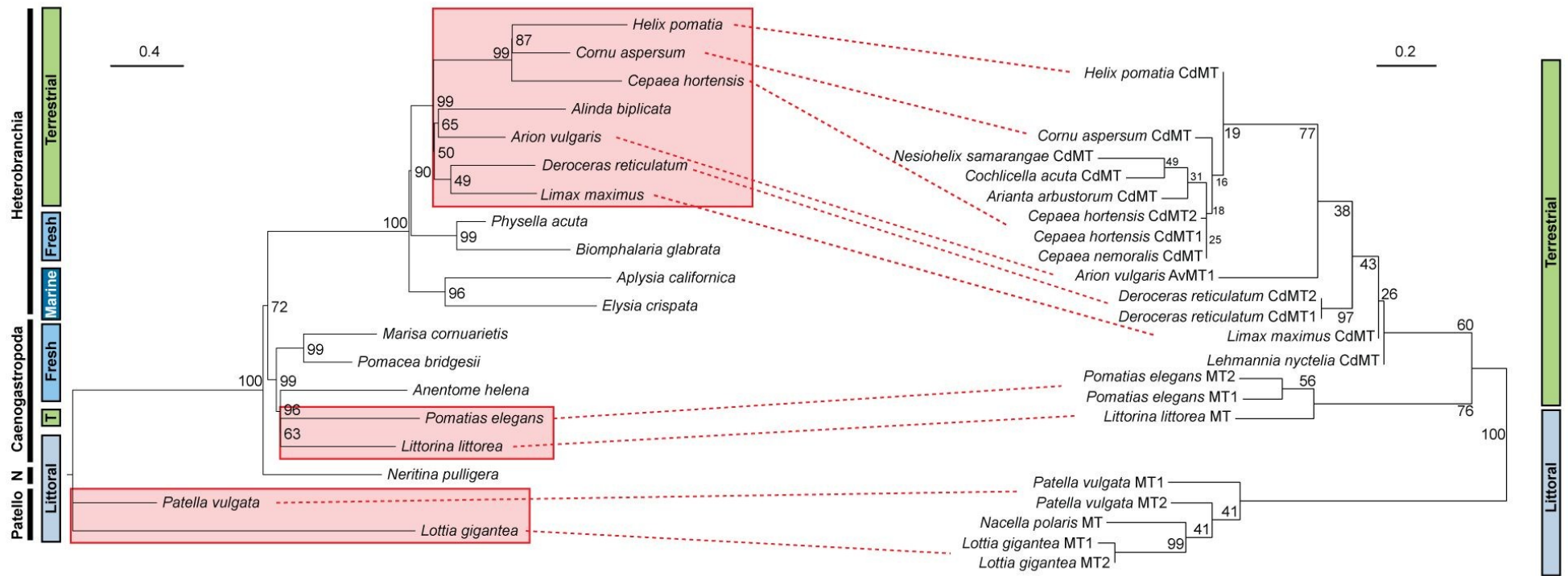


**Figure 6: Mirrored phylogenetic trees (Maximum Likelihood) of investigated species of the four major gastropod clades of Patellogastropoda, Neritimorpha, Caenogastropoda and Heterobranchia.** Right: phylogeny (Maximum Likelihood) showing the separated lineage clusters of only Cd-selective MTs. Bootstrap values (500 replicates) are given at nodes. Left: neutral marker phylogeny based on concatenated COI-18S rDNA data. Bootstrap values (1000 repetitions) are given at nodes. Mirrored species possessing Cd-selective MTs are shown within red-colored frames. Identical species between the two mirroring trees are connected by dotted red lines. On outside margins of the trees, habitats of the represented species are shown with colored bars. On the left outer margin of the neutral marker tree, major taxonomic clades are indicated by black bold lines. Abbreviations: T, Terrestrial; Fresh, Freshwater; Patello, Patellogastropoda; N, Neritimorpha.

984

985

986

987

988

989

990

991

992

993

994

995

996

997

998

999

1000

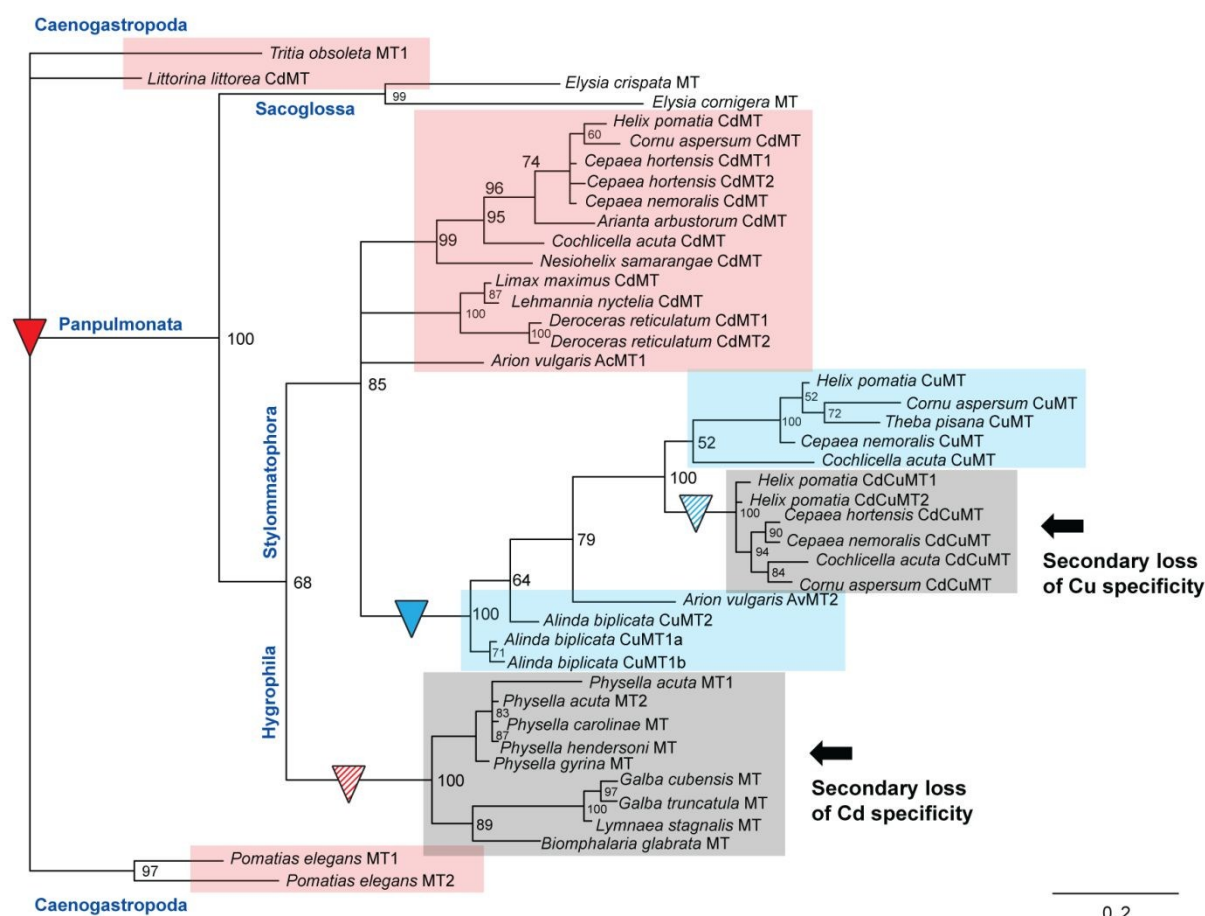


**Figure 7: Bayesian Inference tree with posterior probabilities of metal selectivity features in MTs of Panpulmonata (a taxon of Heterobranchia) versus Caenogastropoda.** Shown are the gain of Cd selectivity (red triangle) in MTs at the root of Caenogastropoda and Heterobranchia, with species possessing Cd-selective MTs underlaid in pink, and the gain of Cu selectivity (blue triangle) in MTs of Stylommatophora, with species possessing Cu-selective MTs underlaid in blue. Also illustrated are the secondary loss of ancestral Cd selectivity in MTs of Hygrophila (red hatched triangle), and the secondary loss of Cu selectivity (blue hatched triangle) in CdCuMTs of Stylommatophora, with respective species clusters underlaid in blue. Bayesian inference calculations were made based on a manually edited MUSCLE alignment (see **alignment S4**) using the free software MrBayes (see Material and Methods).



**Figure 8: Phylogenetic tree (A) and chronogram (B) of Cd and Cu selectivity gain and loss in metallothioneins of Gastropoda.** **A** (inset), phylogenetic tree of Gastropoda (reconstructed after <sup>41,43</sup>) with most probable relationships of gastropod clades (Patellogastropoda, Vetigastropoda, Neritimorpha, Caenogastropoda and Heterobranchia), rooted against the Gastropod sister class of Bivalvia (mussels) <sup>92</sup>. Gain of Cd and Cu selectivity is indicated by red and blue triangles. The kind of metal selectivity in Neritimorpha MTs is still unknown. The possible gain of Zn selectivity in Bivalvia is indicated by an orange triangle with a query. Approximate divergence times (with references) of gastropod lineages are given in million years. Marine (M), littoral (L), freshwater (F) and terrestrial (T) habitats are specified in colored framed boxes. Metal selectivities are indicated by red (Cd-selective), blue (Cu-selective), orange (Zn-selective) and black (unselective) bars. **B** Chronogram showing gains and losses of metal selectivity in MTs of the two gastropod sister clades Caenogastropoda and Heterobranchia (enhanced from grey area in **A**), with their splits into major lineages, including investigated species. Cd-selective MTs (red triangle) appeared prior to the divergence of Caenogastropoda and Heterobranchia, and Cu selectivity (blue triangle) in MT isoforms of Stylommatophora. Cu selectivity was lost in novel MT isoforms of Stylommatophora (hatched blue triangle), and Cd selectivity was lost (hatched red triangles) in freshwater lineages of Ampullariidae (Caenogastropoda) and Hygrophila (Heterobranchia). Approximate divergence times of gastropod lineages are given in million years ago. Grey bars indicate published mean values for the divergence times (references a – e). Vertical, grey dashed lines indicate four of the major mass extinction events. Elevated levels of toxic metals (including Cd) are indicated in grey boxes (references 1 – 6) above the time axis. Chronogram construction was based on: a, <sup>41</sup>; b, <sup>39</sup>; c, <sup>25</sup>; d, <sup>42</sup>; e, <sup>44</sup>. (Additional references: <sup>40,43,93–95</sup>). Dating of increased volcanic Cd or metal emissions are based on information from the following studies: 1, <sup>60</sup>; 2, <sup>63</sup>; 3, <sup>62</sup>; 4, <sup>58</sup>; 5, <sup>57</sup>; 6, <sup>59</sup>. (Additional references: <sup>2,56</sup>).





View Article Online  
DOI: 10.1039/C9MT00259F

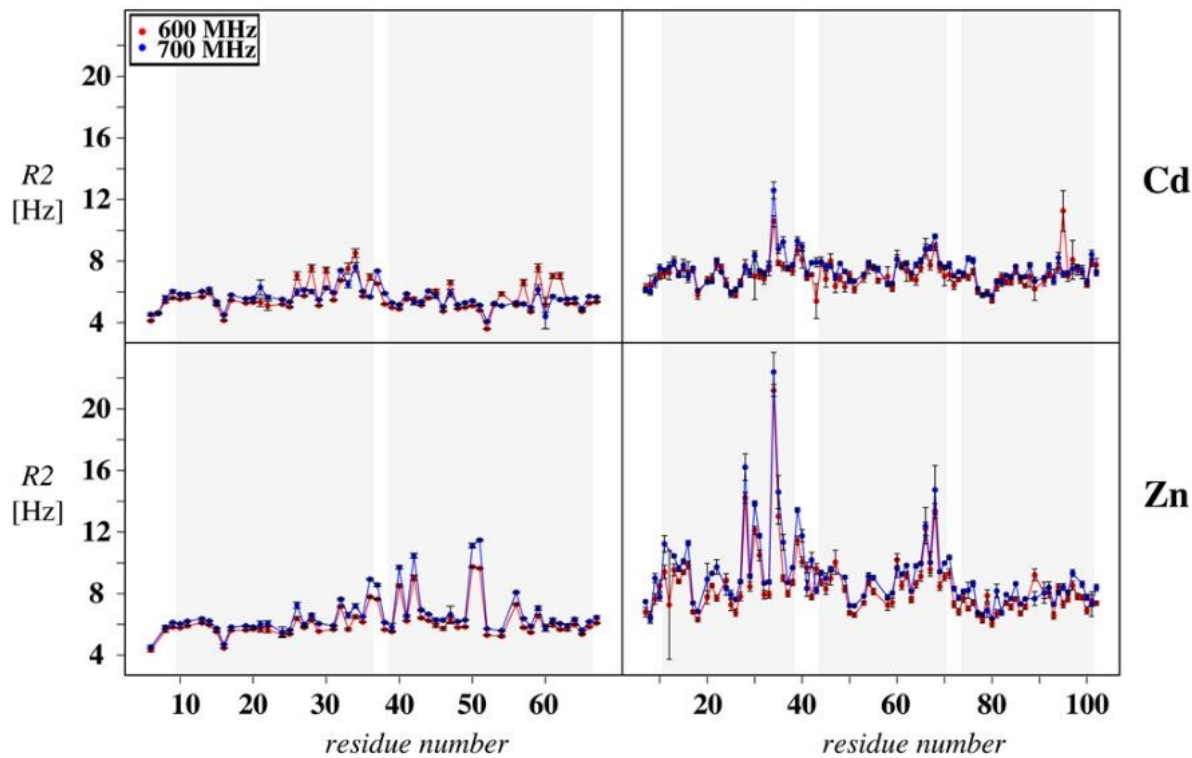


**Figure 9: Conformational exchange effects in MTs.**  $^{15}\text{N}$   $R_2$  rates of the Cd (top) and Zn complexes (bottom) of CdMTs of *Helix pomatia* (left) and *Littorina littorea* (right), recorded at 600 (red) and 700 (blue) MHz. Contributions from conformational exchange can be detected for residues with largely increased  $R_2$  rates.

Metallomics Accepted Manuscript

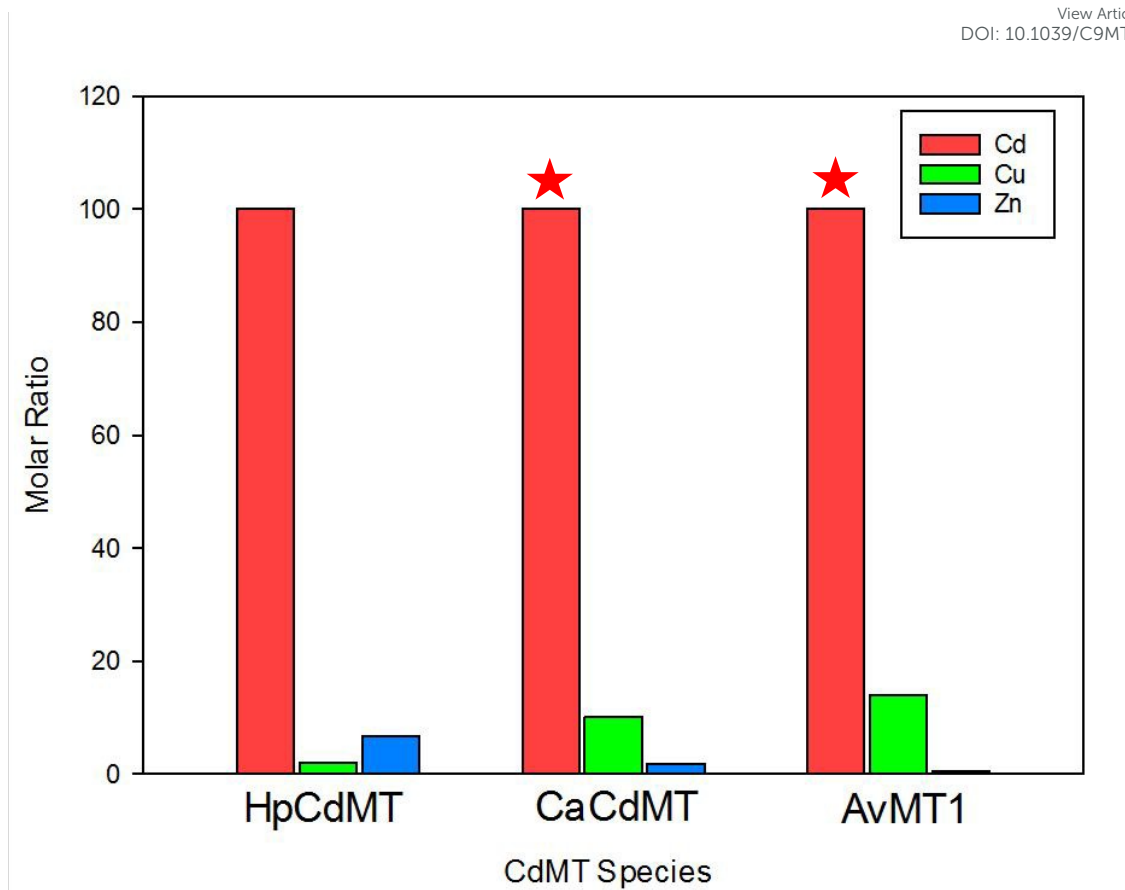
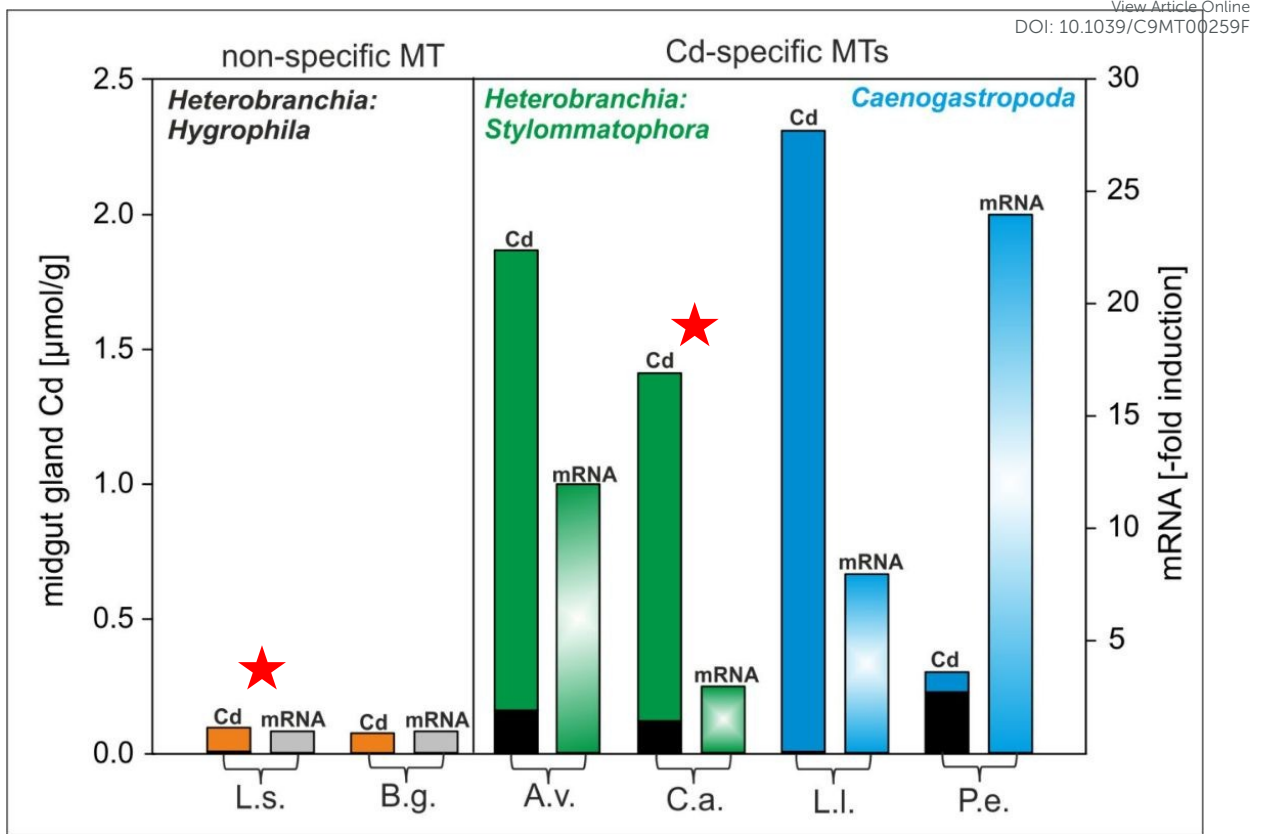


**Figure 10A: Zinc and copper content in native CdMTs isolated from midgut gland preparations of Cd-exposed snails.** Values are given as molar ratios in % of Cd content. HpCdMT, *Helix pomatia* CdMT; CaCdMT, *Cornu aspersum* CdMT; AvMT1, *Arion vulgaris* AvMT1 (CdMT). MTs of species, for which metal contents were analyzed for the first time in this study are marked with a red star. Molar ratios for HpCdMT were re-drawn from data reported in <sup>14</sup>.



Metallomics Accepted Manuscript

**Figure 10B: Cd accumulation and –fold induction of MT gene mRNA transcription in midgut gland of Cd-exposed snails with unselective and with Cd-selective MTs.** Left-hand part of the graph: Cd accumulation (orange bars) and –fold MT mRNA induction (grey bars) in two freshwater snails (*Lymnaea stagnalis* and *Biomphalaria glabrata*, both *Hygrophila*) with unselective MTs. Right-hand part of the graph: Cd accumulation (Cd) and –fold MT mRNA induction for snails possessing Cd-selective MTs, with respective values for *Arion vulgaris* and *Cornu aspersum* belonging to the clade of Stylommatophora (black/green and light green bars), and for *Littorina littorea* and *Pomatias elegans* belonging to the clade of Caenogastropoda (black/blue and light blue bars). Cd contents and mRNA induction data of species analysed de novo for the present study are marked with a red star. The other values were re-drawn from data reported in <sup>96</sup>, <sup>23</sup>, <sup>97</sup> and <sup>16</sup>. Species abbreviations: L.s., *Lymnaea stagnalis*; B.g., *Biomphalaria glabrata*; A.v., *Arion vulgaris*; C.a., *Cornu aspersum*; L.l., *Littorina littorea*; P.e., *Pomatias elegans*.

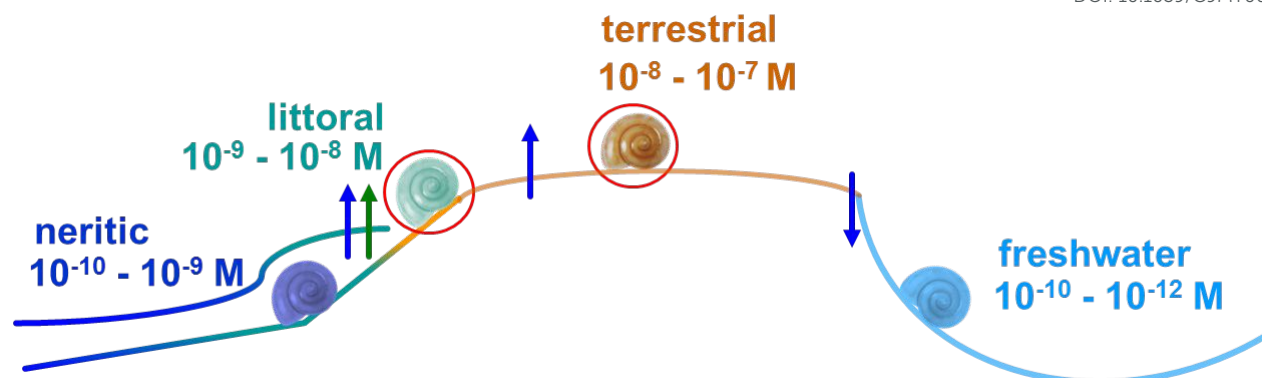


**Figure 11: Molar Cd background concentrations along the axis of evolutionary habitat adaptation in Gastropoda.** Data start from neritic superficial seawater realms, through littoral and terrestrial habitats up to freshwater environments. Blue arrows indicate an increase (upward) or a decrease (downward) of molar Cd concentrations along the habitat axis. The green upward arrow at the transition zone between neritic and littoral habitats symbolizes the increasing availability of Cd due to decreasing concentrations of complexing ligands and decreasing salinity. Snail symbols encircled in red indicate the gain of Cd-selective MTs.



**Table 1** – List of gastropod species and their use for different methodical applications (red check marks) within the present study. Reported are all species acquired (first column) and their utilization for Cd exposure (second column), RNA sequencing and transcriptome assembly (second column), RNA isolation and cDNA transcription (third column), quantitative Real-Time PCR (fourth column), Protein purification from tissues *in vivo* (fifth column), recombinant expression (sixth column), MS analysis (seventh column), NMR analysis and metal titration (eighth column), and construction of neutral marker phylogeny (ninth column).

Animal collection, purchasing and rearing ( <i>Species</i> )	Cd exposure	RNA seq and transcriptome assembly	RNA isolation and cDNA	Quantitative RT-PCR	<i>In vivo</i> protein purification	Recombinant expression	MS analysis	NMR and metal titration	Neutral marker phylogeny
<i>Lottia gigantea</i>			✓			✓	✓		✓
<i>Patella vulgata</i>		✓	✓						✓
<i>Neritina pulligera</i>		✓	✓						✓
<i>Littorina littorea</i>						✓		✓	✓
<i>Pomatias elegans</i>									✓
<i>Marisa cornuarietis</i>			✓						✓
<i>Pomacea bridgesii</i>						✓	✓		✓
<i>Anentome helena</i>		✓	✓						✓
<i>Aplysia californica</i>			✓						✓
<i>Elysia crispata</i>		✓							✓
<i>Physella acuta</i>			✓						✓
<i>Lymnaea stagnalis</i>	✓		✓	✓					
<i>Biomphalaria glabrata</i>									✓
<i>Arion vulgaris</i>					✓	✓	✓		✓
<i>Deroceras reticulatum</i>			✓						✓
<i>Limax maximus</i>									✓
<i>Helix pomatia</i>						✓		✓	✓
<i>Cepaea hortensis</i>			✓						✓
<i>Cornu aspersum</i>	✓		✓	✓	✓				✓
<i>Alinda biplicata</i>		✓	✓						✓